

**COMPARATIVE CALCULATION OF 3-DIMENSIONAL  
SURFACE AREA AND WATER FLOW DIRECTION FROM  
DIGITAL ELEVATION MODELS: A CASE STUDY FOR THE  
AGRICULTURAL LAND IN ESKİSEHİR-CİFTELER  
IRRIGATION**

**SAYISAL YÜKSEKLİK MODELLERİNDEN 3 BOYUTLU  
YÜZEY ALANININ VE SU AKIŞ YÖNLERİNİN  
KARŞILAŞTIRMALI HESAPLANMASI: ESKİŞEHİR  
ÇİFTELER SULAMASI TARIM ARAZİLERİ PİLOT  
UYGULAMASI**

**AYGÜN İREM YAVUZ**

**PROF. DR. ALİ ÖZGÜN OK**

**Supervisor**

Submitted to

Graduate School of Science and Engineering of Hacettepe University

as a Partial Fulfilment to the Requirements

for the Award of the Degree of Master of Science

in Geomatics Engineering

2023

## **ABSTRACT**

# **COMPARATIVE CALCULATION OF 3-DIMENSIONAL SURFACE AREA AND WATER FLOW DIRECTION FROM DIGITAL ELEVATION MODELS: A CASE STUDY FOR THE AGRICULTURAL LAND IN ESKİŐEHİR-ÇİFTELER IRRIGATION**

**Aygün İrem YAVUZ**

**Master of Science, Department of Geomatics Engineering**

**Supervisor: Prof. Dr. Ali Özgün OK**

**June 2023, 57 pages**

The significance of agricultural production and, consequently, numerous agriculture-related parameters are becoming the primary focus of the digitalized world, and with the 2019 pandemic, the significance of food was once again highlighted. In order to ensure the correct and necessary use of water in agriculture, valid surface area values by calculating the irrigated parcel areas in 3-dimensions (3D) are required. The main purpose is to more accurately calculate the amount of water used in irrigation areas on a parcel-by-parcel basis using 3D area values, thereby preventing the plant from receiving insufficient or excessive water. In this way, it is hoped that this will increase efficiency and help prevent losses in agricultural production by ensuring that irrigation calculations are based on accurate area estimates. This thesis compared the calculated area values derived from 3D data to the areas listed on the title deeds for the study area located in the Eskisehir-Cifteler region. To achieve the stated objective, DEMs were obtained from institutions and publicly accessible data sources. In addition, information regarding the DTM's points was obtained from the General Directorate of Land Registry and Cadaster (GDLRC). Utilizing elevation models and parcel data, the 3D measurements of the parcels were obtained. Upon conducting an analysis, it is seen that there is a difference of 235 hectares between the total surface area (GDLRC) and the total title deed area for the selected test site. The area under investigation is a farming community that covers

an estimated total of 10.677,05 hectares. Compared to the total area, the difference might be underestimated; however, considering the country level, it was found to be at a level that could potentially cause substantial agricultural discrepancies.

Keywords: DEM, 3D Surface Area, Title Deed, 3D Cadaster, Irrigation, Agriculture

## ÖZET

# SAYISAL YÜKSEKLİK MODELLERİNDEN 3 BOYUTLU YÜZEY ALANININ VE SU AKIŞ YÖNLERİNİN KARŞILAŞTIRMALI HESAPLANMASI: ESKİŞEHİR ÇİFTELER SULAMASI TARIM ARAZİLERİ PİLOT UYGULAMASI

**Aygün İrem YAVUZ**

**Yüksek Lisans, Geomatik Mühendisliği Bölümü**

**Tez Danışmanı: Prof. Dr. Ali Özgün OK**

**Haziran 2023, 57sayfa**

Tarımsal üretimin ve buna bağlı olarak tarımla ilgili çok sayıda parametrenin önemi dijitalleşen dünyanın birincil odak noktası haline gelirken, 2019 pandemisi ile birlikte gıdanın ne kadar önemli olduğunun bir kez daha altı çizilmiş oldu. Tarımda suyun doğru miktar ile gerekli alanlarda kullanımının sağlanabilmesi için sulanan parsel alanlarının 3 boyutlu (3B) olarak hesaplanarak geçerli yüzey alanı olarak bu değerlerin kullanılmasına ihtiyaç duyulmaktadır. Bu çalışmada temel amaç, sulama alanlarında kullanılan su miktarının 3B boyutlu alan değerleri kullanılarak parsel bazında daha doğru hesaplanması ile bitkinin su ihtiyacının yetersiz veya fazla olmasının engellenmesidir. Bu sayede, sulama hesaplamalarının doğru alan tahminlerine dayanmasını sağlayarak verimliliği artırmayı ve tarımsal üretimde kayıpların önlenmesine yardımcı olunması umulmaktadır. Bu tez, Eskişehir-Çifteler bölgesinde yer alan çalışma alanı için 3B verilerden elde edilerek hesaplanan alan değerlerini tapuda listelenen alanlarla karşılaştırmıştır. Belirtilen amaca ulaşmak için kurumlardan ve kamuya açık veri kaynaklarından DEM verileri temin edilmiştir. Buna ek olarak Tapu ve Kadastro Genel Müdürlüğü'nden (TKGM) Dijital Arazi Modeli nokta verisi (DTM points) elde edilmiştir. Yükselik değerleri ile parsel verileri kullanılarak parsellerin 3 boyutlu ölçümlerine ulaşılmıştır. Yapılan analiz sonucunda seçilen test sahası için toplam yüzey alanı (TKGM) ile toplam tapu

alan deęerleri arasında 235 hektarlık bir fark olduęu grlmektedir. İncelenmekte olan alan, tahmini toplam 10.677,05 hektarı kapsayan bir tarımsal faaliyet alanıdır. Toplam alanla karşılaştırıldığında, fark hafife alınabilir; ancak, lke dzeyi gz nne alındığında, potansiyel olarak nemli tarımsal tutarsızlıklara neden olabilecek dzeyde olabileceęi grlmştr.

Anahtar Kelimeler: DEM, 3D Yzey Alanı, Tapu, 3D Kadastro, Sulama, Tarım

## **ACKNOWLEDGEMENTS**

First, I would like to express my gratitude to my supervisor Assoc. Prof. Dr. Ali Özgün Ok, for his dedicated attention and his efforts.

I would like to thank other committee members of my thesis, Prof. Dr. Sultan Kocaman Gökçeođlu, Assoc. Prof. Dr. Zeynel Abidin Polat, Assoc. Prof. Dr. Saygın Abdikan and Asst. Prof. Murat Durmaz for their valuable comments and contributions.

I would like to thank my mother, my father and my husband for their love and valuable support. I am thankful to Mehmet Murat Tuzlacıođlu for his support and assistance.

**Aygün İrem YAVUZ**

**June 2023, Ankara**



# CONTENTS

ABSTRACT .....	i
ÖZET .....	iii
ACKNOWLEDGEMENTS .....	v
CONTENTS .....	vi
LIST OF TABLES .....	viii
LIST OF FIGURES .....	ix
LIST OF ABBREVIATIONS .....	xi
1. INTRODUCTION .....	1
1.1. Purpose and Scope.....	1
1.2. Contributions.....	3
1.3. Organization of the Thesis.....	4
2. BASICS AND STATE-OF-ART .....	5
2.1 Methods for Parcel Area Calculation.....	5
2.2. 3D Cadaster.....	6
2.3. 3D Surface Area Calculation.....	6
2.3.1. Related Work for Surface Area Calculation.....	8
2.4. Calculating Flow Directions.....	9
2.4.1 Related Work for Calculating Flow Diretions.....	10
3. STUDY AREA.....	11
4. DATASET AND PROCESSING.....	14
4.1. The Datasets Obained.....	14
4.1.1 DEM Data.....	16
4.1.2 DTM Points.....	20
4.1.3 Parcel Data.....	21
4.2 Main Processing Steps Involved.....	22
4.2.1 Cloth Simulation Filter (CSF).....	22
4.2.2 Interpolating.....	23
4.3 Calculating Surface Area With DTM.....	24
4.4 Calculating Flow Directions.....	25
4.5 Processed Outputs.....	25



4.5.1 Generating DTM.....	25
4.5.2 Surface Area Calculation.....	35
4.5.3 Flow Direction Outputs.....	36
5. RESULTS AND DISCUSSION.....	38
5.1 Comparisons Using Interpolated Surface Areas.....	38
5.2 Flow Direction Calculations.....	44
6. CONCLUSIONS.....	48
REFERENCES .....	50
APPENDICES.....	55
Attach 1 - Thesis Derived Publications.....	56
CURRICULUM VITAE.....	57

## LIST OF TABLES

Table 4.1	The datasets collected for the related study area.....	15
Table 5.1	Sum of absolute differences calculated in hectares (with gross errors).....	38
Table 5.2	The parcel counts associated with the differences between title deed area and cadastral areas are presented on a village-by-village basis.....	40
Table 5.3	The parcel counts associated with the differences between the surface area and cadastral area.....	41
Table 5.4	Parcel Counts for DEM based differences between Surface area and Title Deed Area.....	41
Table 5.5	Irrigation water values for crops at 15ha in laboratory conditions.....	46
Table 5.6	Irrigation water values for crops at 15 ha in field settings.....	47

## LIST OF FIGURES

Figure 1.1	SuET Interface.....	2
Figure 2.1	Cadastral map produced by graphic method [13].....	5
Figure 2.2	Cadastral map produced by photogrammetric method [13].....	5
Figure 2.3	Error in parcel boundaries measured with classical tachometer [13].....	6
Figure 2.4	Logo of 3D cadasters working group [14].....	6
Figure 2.5	Jenness’s method. [19].....	7
Figure 2.6	Modified method [19].....	7
Figure 2.7	(a)8 triangles for calculation of surface area with summed shaded square region. (b) 4 triangles for calculation surface area with summed shaded square region [23].....	8
Figure 2.8	Flow directions [26].....	9
Figure 2.9	Contour and streams [29].....	10
Figure 3.1	Türkiye-Eskisehir-Cifteler.....	11
Figure 3.2	Overview of the study area (Google Earth Image).....	12
Figure 3.3	Orthomosaic of the study area.....	12
Figure 3.4	Terrestrial images from the selected study area.....	13
Figure 4.1	Processing steps involved.....	14
Figure 4.2	(a) ALOS DSM and (b) ASTER GDEM covering the study area.....	18
Figure 4.3	EUDEM (25m) covering the study area.....	18
Figure 4.4	SRTM DEM (30m) covering study area.....	19
Figure 4.5	DEM from General Directorate of Mapping (5m).....	19
Figure 4.6	DEM from Sakaryabasi Irrigation Union Presidency (5m).....	20
Figure 4.7	DTM Points with study area.....	21
Figure 4.8	DTM generated from points using interpolation.....	21
Figure 4.9	Parcel data utilized.....	22
Figure 4.10	Generating DTM from DEM with CSF [47].....	22
Figure 4.11	Principle of CSF [47].....	23
Figure 4.12	Point cloud of GDLRC DTM points.....	26
Figure 4.13(a)	Input point cloud of EuDEM.....	26
Figure 4.13(b)	Automatically extracted ground points of EUDEM.....	26

Figure 4.13(c)	Automatically extracted off-ground points of EUDEM .....	27
Figure 4.14(a)	Input point cloud of GDM DEM.....	27
Figure 4.14(b)	Automatically extracted ground points of GDM DEM.....	27
Figure 4.14(c)	Automatically extracted off-ground points of GDEM.....	27
Figure 4.15(a)	Input point cloud of SIUP DEM.....	28
Figure 4.15(b)	Automatically extracted ground points of SIUP DEM.....	28
Figure 4.15(c)	Automatically extracted off-ground points of SIUP DEM.....	28
Figure 4.16(a)	Input point cloud of ALOS DEM.....	28
Figure 4.16(b)	Automatically extracted ground points of ALOS DEM.....	29
Figure 4.16(c)	Automatically off-ground points of ALOS DEM.....	29
Figure 4.17(a)	Input point cloud of ASTER DEM.....	29
Figure 4.17(b)	Automatically extracted ground points of ASTER DEM.....	29
Figure 4.17(c)	Automatically extracted off-ground points of ASTER DEM.....	30
Figure 4.18(a)	Input point cloud of SRTM DEM.....	30
Figure 4.18(b)	Automatically extracted ground points of SRTM DEM.....	30
Figure 4.18(c)	Automatically extracted off-ground points of SRTM DEM.....	30
Figure 4.19	GDLRC DTM Points that Intersect with Study Area (Count 369.959).....	31
Figure 4.20	ALOS DTM Points (15.870 Ground Points).....	31
Figure 4.21	ASTER DTM Points (2.313 Ground Points).....	31
Figure 4.22	EUDEM DTM Points (27.230 Ground Points).....	32
Figure 4.23	GDM DTM Points (4.357.709 Ground Points).....	32
Figure 4.24	SRTM DTM Points (11.564 Ground Points).....	32
Figure 4.25	SIUP DTM Points (3.841.321 Ground Points) .....	32
Figure 4.26	The orthophoto has been overlaid with GDM ground points.....	33
Figure 4.27	The orthophoto has been overlaid with SIUP ground points.....	33
Figure 4.28	The orthophoto has been overlaid with EUDEM ground points.....	34
Figure 4.29	The orthophoto has been overlaid with SRTM ground points.....	34
Figure 4.30	The orthophoto has been overlaid with ALOS ground points.....	34
Figure 4.31	The orthophoto has been overlaid with ASTER ground points.....	35
Figure 4.32	The orthophoto has been overlaid with GDLRC ground points.....	35
Figure 4.33	Parcel Data with DEM from DTM Points.....	36
Figure 4.34	Flow direction with D8 Method.....	36
Figure 4.35	Flow direction with MFD Method.....	37
Figure 4.36	Flow direction with DINF Method.....	38

Figure 5.1	Surface area and title deed area absolute differences classes for ALOS.....	42
Figure 5.2	Surface area and title deed area absolute differences classes for ASTER...	42
Figure 5.3	Surface area and title deed area absolute differences classes for EUDEM....	42
Figure 5.4	Surface area and title deed area absolute differences classes for GDM.....	43
Figure 5.5	Surface area and title deed area absolute differences classes for SRTM.....	43
Figure 5.6	Surface area and title deed area absolute differences classes for SUIP.....	43
Figure 5.7	Surface area and title deed area absolute differences classes for DTM points DEM.....	44
Figure 5.8	Flow Accumulation MFD Method.....	45
Figure 5.9	Flow accumulation with parcel data.....	45

## LIST OF ABBREVIATIONS

SuET	The irrigation management and crop water consumption
AR	Augmented reality
2D	Dimensional
3D	3-Dimensional
DEM	Digital Elevation Model
DTM	Digital Terrain Model
DSM	Digital Surface Model
SFM	Structure From Motion
GIS	Geographical Information System
GPS	Global Positioning System
BIM	Building Information Model
FIG	Federation of Surveyors
FVDS	Flow velocity and direction system
LADM	Land Administration Domain Model
LIDAR	Light Detection and Ranging
TIN	Triangulated Irregular Network
GDM	General Directorate of Mapping
ALOS	Advanced Land Observing Satellite
ASTER	Advanced Spaceborne Thermal Emission and Reflection Radiometer
EUDEM	European Digital Elevation Model
SRTM	Shuttle Radar Topography Mission
GDLRC	General Directorate of Land Registry and Cadaster
CSF	Cloth Simulation Filter
IDW	Inverse Distance-Weighted
MFD	Multiple Flow Direction
SIUP	Sakaryabasi Irrigation Union Presidency



# 1. INTRODUCTION

## 1.1. Purpose and Scope

Title deeds are the official documents in regards to ownership and area, as they detail the exact boundaries of a property. The area values on title deeds are utilized for real estate finance, expropriation, agricultural input calculations, and support payments, among other purposes. [1] Old technologies and human error have introduced inaccuracies into many of the estimates conducted over different regions. Additionally, the areas are measured in two dimensions (2D) while conducting cadastral studies in the field. Measurements taken in this manner do not allow for the accurate calculation of areas that originate from the earth's rugged land regions. Accessing digital elevation data from spaceborne, airborne, and drones is made easier by modern technology, which also facilitates the calculation of areas including surface variations in three-dimensions (3D).

Due to the discrepancies between registered and geometric areas, it is well known that numerous legal disputes occur in our country. Türkiye has 120.251 parcels with an area difference greater than 100% and 372.427 parcels with an area difference greater than 50% [2]. In other words, while it is evident that there are differences between the geometric area and the surface area around the world, it is revealed that these differences will be even more prominent in Türkiye. Thus, it is expected that applications that employ registered area values for various transactions may generate incorrect results.

These days, cadastral research and 3D applications are quite popular, although these studies deal with significant concentrations of buildings, such as certain high-rise structures [3, 4]. A few research studies are also being conducted on marine 3D cadasters in order to develop a marine model for the management of maritime areas, e.g. [5]. Those studies are dependent on buildings, maritime or engineering structures such as bridges, highways, etc., and they examined high or low above-ground locations. For a 3D cadaster system, they employed Geographical Information System (GIS), Augmented Reality (AR), and other 3D methods to determine ownership of assets that are not at ground level.

This thesis examined land surface area in order to calculate the actual parcel area for agricultural irrigation purposes. There is a notable distinction between areas computed



from 2D planar and 3D surfaces [6]. For instance, farmers receive subsidies for the products they produce on their own fields; however, these areas are computed from 2D cadastral parcels; therefore, if the field area has uneven topography and the parcels are not estimated as 3D surface area, the amount paid to farmers is decreased. Consequently, the amount that should be reflected in the farmers' income will fall. In reality, though, a farmer will have received less support than she or he should have, despite having planted more fields and invested more resources.

For irrigation, farmers utilize water determined based on the unit areas of their crops. If these regions also have uneven characteristics, the estimated amount of water may be lower for certain parts of the region, and the plants in that region will receive less water. Accordingly, the yield of the crop will fall, and if we consider the entire country, the yield and food that will be supplied will eventually decrease for the entire population.

As depicted in Figure 1.1, the irrigation management and crop water consumption (SuET) tool developed by the Ministry of Agriculture and Forestry to calculate irrigation amounts was also made available to farmers [7]. The arithmetic of crop water requirement (ET crop) is dependent on a number of variables, such as climate conditions, especially times of effective rainfall and dry periods, the plant's own water requirement capacity (which can vary from crop to crop), soil structure, humidity, sunshine, wind speed, vegetative times, etc. [8, 9]. In order to compute the water demand for the entire parcel, it is necessary to determine the parcel's area after being aware of these facts.

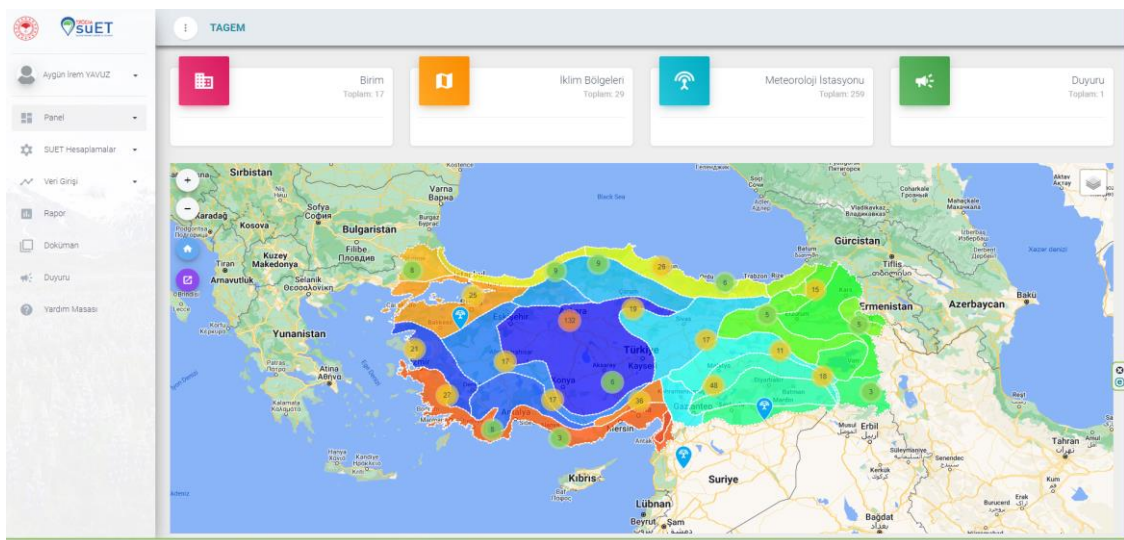


Figure 1.1. SuET Interface

Also, determining the flow directions of water is a crucial issue for agriculture and urban development. Accurately calculating the slope areas enables the identification of locations where water accumulates, the facilitation of irrigation planning in agriculture, and the prevention of flooding and sludge in urban landscapes.

Despite the inaccuracies in Digital Elevation Model (DEM) data, studies have been carried out to calculate real surface areas, as described in the literature [9, 10, 11]. There are free DEM data with a coarse ground sampling distance (GSD) (e.g., 30 m–90 m) available via the internet, and many authorities in Türkiye, notably the General Directorate of Mapping of Türkiye, produce DEM data (e.g., at 5–30 m GSD). The General Directorate of Land Registry and Cadaster (GDLRC) of the Ministry of Environment, Urbanism, and Climate Change also produces Digital Terrain Model (DTM) points and associated orthoimages. In this thesis, such data and an additional elevation model with a 5 m GSD obtained from the Sakaryabasi Irrigation Union Presidency are compared with official parcel boundaries and registered area values obtained from the same source (i.e., SIUP).

Obtaining DTM data by eliminating objects such as trees, crops, and buildings from DEM data is an important aspect of this thesis's topic. This critical aspect allows the calculation of accurate surface area and flow directions since there is a significant difference between computing surface area with and without pixels with abrupt height fluctuations. Also, it makes sense to exclude crop heights when estimating flow directions. Therefore, generating valid DTM data is essential for obtaining precise surface area and flow directions.

## **1.2. Contributions**

This thesis involves the computation of surface area and flow directions of parcels with 3D information, utilizing comparative data such as DEM data with varying resolutions. Furthermore, a comparative analysis was carried out to investigate the relationship between surface area and the aim of optimizing water usage in agriculture, demonstrating that the appropriate amount of water is utilized. This study highlights the importance of the careful utilization of water resources, which is known to be a crucial factor in enhancing crop productivity. Furthermore, the computation of 3D surface areas and the subsequent comparison with 2D areas may serve to increase awareness of other types of

area-based analyses, such as support payments, the process of fertilization, real estate finance, and country-based area assessments.

### **1.3. Organization of the Thesis**

This thesis is structured into five distinct sections. The second section of this thesis elaborates on various techniques for determining parcel area, investigations into 3D cadaster, relevant literature, and procedures for flow calculations. Framework for the study, including the study area, comparing DEM data, creating DTM, calculating surface area, flow directions and strategies, and the dataset used, detailed in sections three and four. The findings of the research, as well as the discussions and conclusions, are presented in sections five and six of the thesis.

## 2. BASICS AND STATE-OF-ART

### 2.1 Methods for Parcel Area Calculation

Land parcel area calculations are typically performed for real estate purposes. While performing these computations on the ground, various methodologies are employed. Digital Cadaster, Classical Cadaster, and Photogrammetric Cadaster (Figure 2.2) are types of regularly employed existing studies for valuing land using graphical/terrestrial (Figure 2.1), aerial imagery, or electronic and GPS (Global Positioning System) devices [12, 13]. As shown in Figure 2.3, all of these measurements are susceptible to inaccuracy due to the inadequacies of the techniques used to convert the 3D earth surface to the 2D paper environment. Area is calculated using 2D methods that neglect topography and surface roughness. Thus, it is evident that 2D approaches cannot accurately represent the area of parcels on the actual earth's surface.



Figure 2.1. Cadastral map produced by graphic method [13]

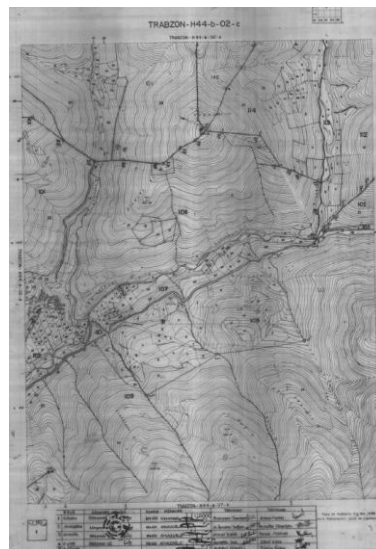


Figure 2.2. Cadastral map produced by photogrammetric method [13]

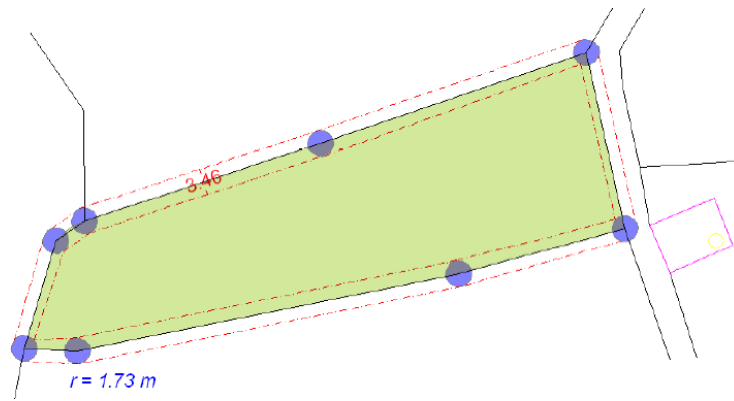


Figure 2.3: Error in parcel boundaries measured with classical tachometer [13]

## 2.2 3D Cadaster

Typically, a 3D cadaster is performed on the areas and property rights of multi-story or high-rise structures in urban areas. This is a requirement for the increasing population and the Building Information Model (BIM) relative to the Land Administration Domain Model (LADM). Due to the inadequacies of the 2D cadaster in terms of rights and responsibilities, 3D cadastral research is necessary. For 3D cadasters, the International Federation of Surveyors (FIG) has already established a working group (Figure 2.4) [14, 15, 16, 17].



Figure 2.4. Logo of 3D cadasters working group [14]

## 2.3 3D Surface Area Calculation

Many methods can be used to determine the total surface area based on a DEM. A digital elevation model is a numerical and digital representation of the elevation of the ground surface relative to any reference surface or coordinate system. It reflects the surface's topography [18]. The DEM models are subdivided into the Digital Surface Model (DSM) and the DTM. DSM is the surface model that includes the height of every feature on the surface, while DTM is the model of the earth's surface without the height of any other objects. DTM is required to accurately calculate surface area. Because the elevation data of trees, buildings, and other taller objects induce errors in calculating surface area, 3D surface area will always be greater than planar area [19].

Surface models can be obtained using LiDAR, photogrammetric images from aircraft, applications that utilize camera images such as Structure from Motion (SFM) [20], and other software compatible with drone cameras at finer resolutions or for free from websites with coarse resolutions.

Generally, surface area is calculated by dividing DEM pixels into eight 3D triangles. Throughout the process of these investigations, eight three-dimensional triangle models are utilized, in which eight surrounding cells are connected to the center point, the cell areas within the triangle are computed, and the total area is determined (Figure 2.5). By modifying this method, experimenting with interpolation techniques, and comparing the findings with LiDAR data [21], new methods, such as using 16 nearby pixels to calculate surface area, were revealed (Figure 2.6).

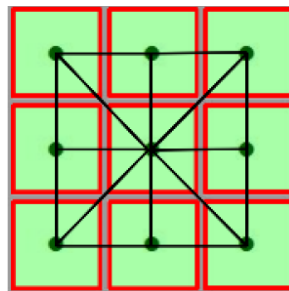


Figure 2.5. Jenness's method. [19]

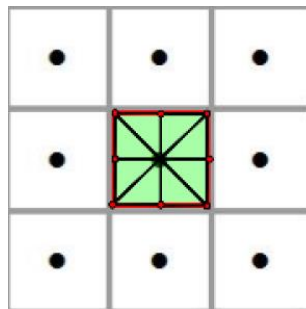


Figure 2.6. Modified method [19]

According to [21], this method has significantly less accuracy than the Triangulated Irregular Network (TIN) method when calculating surface area statistics. Using the continuous surface area derived from DEM data and the TIN, surface area calculations are also performed. Rather than calculating raster data area, vector area is calculated. However, this calculation depends on the accuracy of the DEM data. Hence, there are

measuring errors. To reduce bias, a 2<sup>nd</sup> order bias correction is recommended. This method employs a probability integral incorporating the Monte Carlo method. However, this method is computationally intensive and requires the distribution of DEM errors [22]. Utilizing DEM data to calculate surface area demonstrates the importance of scale and resolution. In addition, interpolation methods are essential for precisely determining the surface area [22].

Light Detection and Ranging (LiDAR) measures have more precise and high-resolution data to determine the actual surface area, but they require more time for data production and calculations as well as large data storage.

Calculations of surface area were possible by dividing the area into squares, rectangles, and triangles; first- and second-order derivatives of land surface were estimated for debugging DEM errors using the least squares approach together with the DEM data (Figure 2.7). It was found that this method is more reliable than TIN methods [22,23,24].

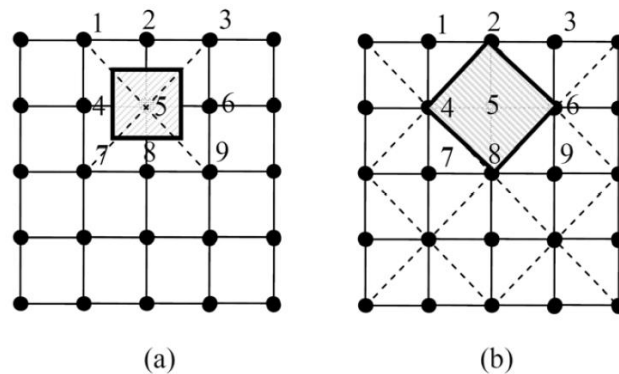


Figure 2.7. (a) 8 triangles for calculation of surface area with summed shaded square region. (b) 4 triangles for calculation surface area with summed shaded square region [23].

### 2.3.1 Related Work for Surface Area Calculation

Land measurements are time-consuming, and determining the surface area of large regions requires DEM data and real polygon boundaries for comparison with the land measurements. DEM datasets with various resolutions are freely available on the internet. Moreover, DEM data comparisons are required for determining how DTM generation outputs and surface area changes perform across varying DEM resolutions.

In these scenarios, there are two surface area-related questions to answer:

- Does the difference between 2D planar area and 3D surface area have a significant impact?
- How much do DEM resolutions affect the discrepancies between 2D planar area and 3D surface area?

The results of this study may provide an answer to the first question, demonstrating that the subject depends on the settings in which it is studied. This research fills a gap in the literature by providing real-world vector data that has previously been lacking in agricultural studies. This thesis also provides an explanation for the second question that has not been addressed frequently in the literature.

## 2.4 Calculating Flow Directions

Determining where water tends to accumulate is useful information when planning irrigation. This is one of the parameters influencing the plant's water uptake. As depicted in Figure 2.8, flow directions could be determined to calculate this requirement. It is essential to differentiate across areas with and without water accumulation as a result of factors such as precipitation and irrigation. This is also useful for determining the flow directions in order to identify the areas where soil minerals will be collected by the water flow.

Although elevation values are utilized in land measures, DEMs consisting of these values have been used for a long time to calculate flow direction [25-30].

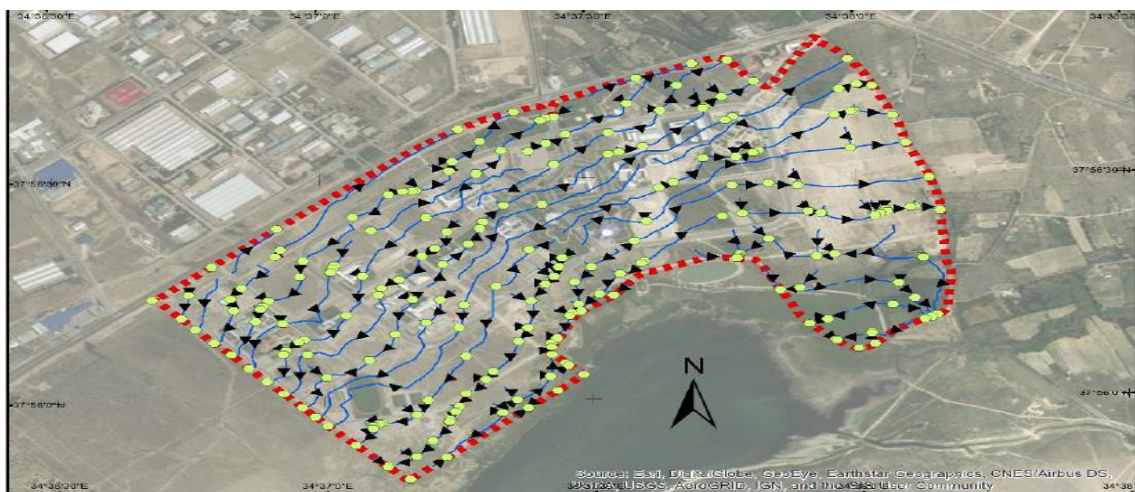


Figure 2.8. Flow directions [26]



### 2.4.1 Related Work for Calculating Flow Directions

The Flow Velocity and Direction System (FVDS), which is a device for generating hydrodynamic pressure samples at various control locations, is used to get accurate hydrodynamic pressure information along with slope data [31].

Directions of flow can be determined using grid and TIN representations of DEM data [25-30]. As a grid system, 8 triangular facet-centered grid points are employed to calculate 8 potential orientations in DEM data [32]. There are software codes and software tools designed for flow direction calculations, and these can be utilized to perform mathematical calculations. These computations additionally make use of DEM data as well as contour and TIN-based solutions via a software interface (Figure 2.9).

Flow direction calculations could be performed using methods of machine learning. The use of DEM data with different resolutions could be beneficial to machine learning studies [30].

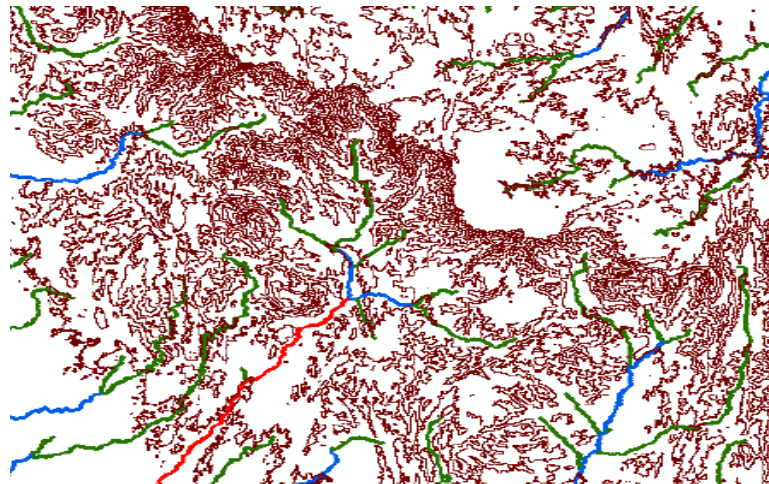


Figure 2.9. Contour and streams [29]

### 3. STUDY AREA

This section of the thesis will provide an in-depth description of the study area that was subject to investigation.

The study area under consideration is located in Eskisehir-Cifteler, as depicted in Figure 3.1. Cifteler is a municipality and district in the province of Eskisehir in the Turkish region of Central Anatolia. The population of the district was recorded at 16.716 in the 2000 census, with 11.872 of those people residing in the town of Cifteler. The region under consideration relates to the irrigation zone of Cifteler, Eskisehir, encompassing a total of eleven villages. The entire district spans around 820 square kilometers at an average elevation of 875 meters. Turbanhe region in question exhibits an average temperature of 11°C and an average precipitation of 360 mm. The soil structure is predominantly composed of brown soil with a medium loam texture. The agricultural land use capability value is generally classified as Class II. The area is known for producing a variety of crops, including barley, wheat, corn, and sunflowers [33, 34]. Ease of access to the data was taken into account in the selection of the study area.



Figure 3.1: Türkiye-Eskisehir-Cifteler

The study area falls under the responsibility of the Sakaryabasi Irrigation Union Presidency, as illustrated in Figure 3.2. The entire land area (2D) of this region measures approximately 15.444,6792 hectares, which is precisely equivalent to 154.446.791,803 square meters. The study area, along with orthophotos, is depicted in Figure 3.3.



Figure 3.2. Overview of the study area (Google Earth Image)



Figure 3.3. Orthomosaic of the study area

The topography of the study area appears to be relatively flat, as depicted in Figure 3.4. The significance of this data lies in its importance to the investigation of differences between 2D and 3D geographic areas. It is possible to approximate that the magnitude of this difference will be diminished in flat topographies and amplified in uneven topographies.





Figures 3.4. Terrestrial images from the selected study area.

## 4. DATASETS AND PROCESSING

This section encompasses the datasets utilized in the study as well as an analysis of the methodology and processing steps employed. The investigation was conducted utilizing data pertaining to the responsibility area of the SIUP in Eskisehir-Cifteler.

This section includes the following steps as shown on Figure 4.1:

- Obtaining DEM data with different resolutions,
- Processing DEM data for generating DTM data,
- Calculating surface area of each polygon,
- Comparing the surface area, registered area and planar area of the polygons,
- Calculating flow directions over the DTM,
- Obtaining flow accumulations from flow directions and matching them with parcels.

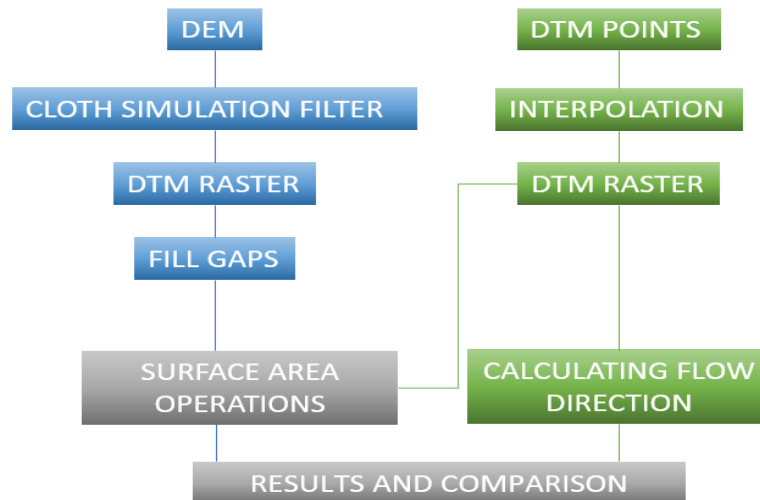


Figure 4.1. Processing steps involved.

### 4.1 The Datasets Obtained

DEM datasets with varying resolutions are used to compute and compare surface areas, flow directions, and accumulations. However, it should be noted that DTM data is required for precise calculations. Therefore, successfully creating DTM data is another component of this study. Once the DTM data and polygonal boundaries were collected, determining surface areas and flow directions became possible.

Relatively low-resolution DEM data were downloaded from publicly accessible data repositories. Relatively high-resolution DEM data is obtained from official sources. The DEM data obtained from SIUP have a resolution of 5 meters, and the GDM DEM data have the same resolution. Spaced every 20 meters, DTM information was collected by the General Directorate of Land Registry and Cadaster (GDLRC). Surface area is calculated using DEM data and land measurements, and the results are compared.

Besides, polygon vector data representing parcel-based information has been retrieved from SIUP. All of the related data information is summarized in Table 4.1 and explained in detail in the following part. Note also that all the datasets presented in Table 4.1 were processed by open-source Cloud Compare software that can be obtained freely from the web and ArcGIS software.

Table 4.1. The datasets collected for the related study area.

<b>Data</b>	<b>Data Type</b>	<b>Data Resolution / Scale</b>	<b>Horizontal Accuracy</b>	<b>Vertical Accuracy</b>	<b>Source</b>
DEM	Raster	5m	±30cm	±3 m at the 90% confidence interval	GDM
DEM	Raster	5m	x = 8,5 cm y = 9 cm	±1,96 m at the 95% confidence interval	SIUP
DEM	Raster	25m	5 m at the 95% confidence interval	±2,9 m at the 95% confidence interval	EUDEM
DEM	Raster	30m	±5 m at the 90% confidence interval	±5 m at the 90% confidence interval	ALOS
DEM	Raster	30m	±30 m at the 95% confidence interval	±20 m at the 95% confidence interval	ASTER
DEM	Raster	30m	±15 m at the 90% confidence interval	±10 m at the 90% confidence interval	SRTM
Orthophoto	Raster	30cm		-	GDLRC
DTM	Point	1/5000 – 20m spaced-out	3 cm	5 cm	GDLRC
Parcel	Vector	1/5000		-	SIUP

#### 4.1.1 DEM Data

This thesis makes use of three different types of DEM datasets. The first form has a low resolution but is freely available online (i.e., ALOS DSM, ASTER GDEM, EUDEM, and SRTM DEM); the second form is obtained from government institutions (i.e., GDM and SIUP DEMs); and the third form is generated from DTM points using an interpolation method (i.e., GDLRC DEM).

Figure 4.2 (a) displays the Advanced Land Observing Satellite (ALOS) DSM and the study area with a resolution of 30 m, utilizing the WGS 1984 coordinate system measured in degrees (EPSG 4326). ALOS platform operated from 2006 to 2011. The Japan Aerospace Exploration Agency (JAXA) published the ALOS DSM as a global digital surface model on 2016. JAXA generated this data as  $1^\circ \times 1^\circ$  tiles of 1 arc sec ( $\sim 30$  m) by resampling the 5 m ALOS DEMs, and utilized the panchromatic stereo mapping sensor (PRISM) on the ALOS platform. The dataset has 5 m Root Mean Square (RMS) value without any ground control points (GCPs) [35, 36].

Figure 4.2 (b) shows the Advanced Spaceborne Thermal Emission and Reflection Radiometer (ASTER) Global Digital Elevation Model (GDEM) of the study area with the same 30 m resolution and with the same coordinate system. In 2019, a consortium consisting of the Ministry of Economy, Trade, and Industry (METI) of Japan and the United States National Aeronautics and Space Administration (NASA) announced the release of the ASTER GDEM. The first version of ASTER GDEM was generated through the utilization of stereo dual images obtained by the ASTER instrument aboard the Terra satellite. The dataset encompasses a range of 83 degrees north latitude to 83 degrees south latitude, providing coverage for approximately 99 percent of the Earth's land area. Upon analysis of the ASTER Global Digital Elevation Model (DEM) Validation Summary Report, it was determined that the vertical data exhibited an accuracy of 20 meters at a 95% confidence level, while the horizontal data displayed an accuracy of 30 meters at a 95% confidence level. According to a literature review, a study conducted in various regions of Türkiye has reported an accuracy range of 9-12 meters [37, 38].

The EUDEM, which has a spatial resolution of 25 meters, is depicted in Figure 4.3. The study area is situated within the ETRS 1989 LAEA coordinate system (EPSG 3035). The EU-DEM is a digital representation of the surface model (DSM) offered by the

Copernicus Land Monitoring Service, which accurately depicts the first surface that is illuminated by different sensors. The product is a hybrid, utilizing a weighted average methodology that incorporates data from the Shuttle Radar Topography Mission (SRTM), ASTER GDEM, and Russian topographic maps. The vertical accuracy value is 2,9 meters in general but for Türkiye it is 2,56 meters [39, 40].

Figure 4.4 illustrates the study area and SRTM DEM, which were measured in degree units on the WGS 1984 coordinate system with a resolution of 30 m (EPSG 4326). The product known as SRTM is the result of a collaborative effort between the National Geospatial-Intelligence Agency (NGA) and the National Aeronautics and Space Administration (NASA). The employed methodology involves the use of radar interferometry. The Shuttle Radar Topography Mission (SRTM) was comprised of a pair of radar antennas. One of the aforementioned entities was situated within the payload bay of the shuttle, while the other was situated at the terminus of a 200-foot mast that extended from the payload bay. The satellite in question has gathered information pertaining to 80% of the Earth's surface. The minimum value for absolute vertical height accuracy is 16 m, while the minimum value for relative vertical height accuracy is 10 m. Additionally, the minimum value for absolute horizontal circular accuracy is 20 m. Within the realm of literature research, several studies have been conducted in Türkiye that encompass various study areas. These studies have revealed that the accuracy value for 90% of the country falls below 9 meters [41-43].



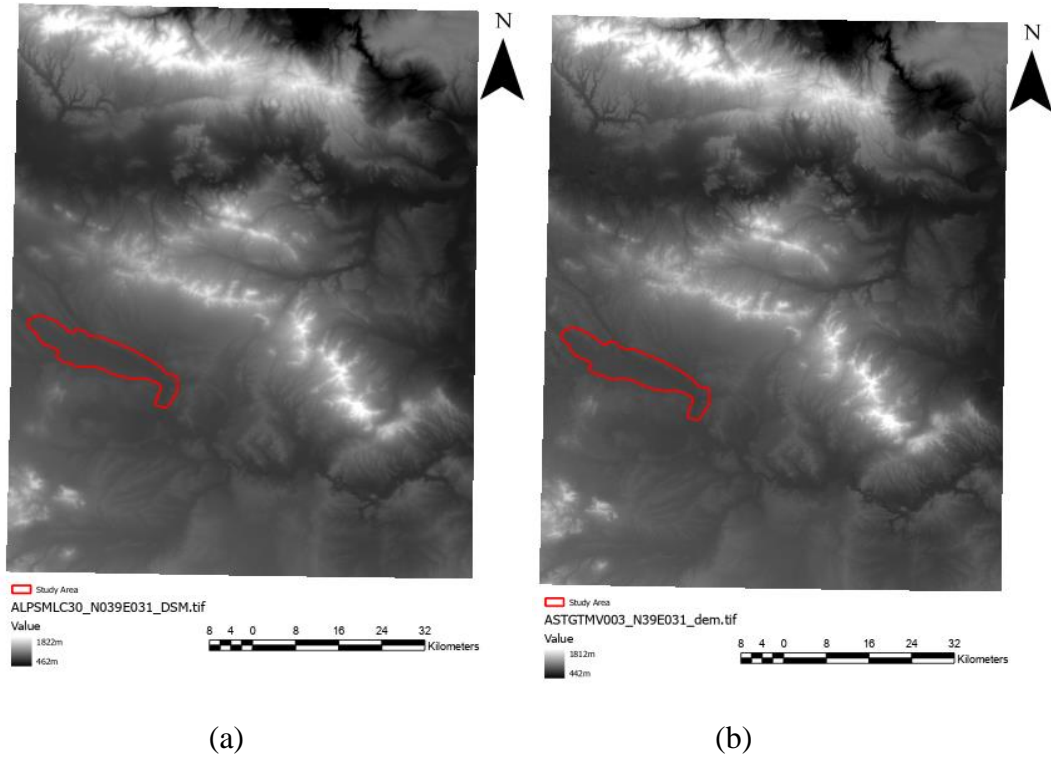


Figure 4.2. (a) ALOS DSM and (b) ASTER GDEM covering the study area

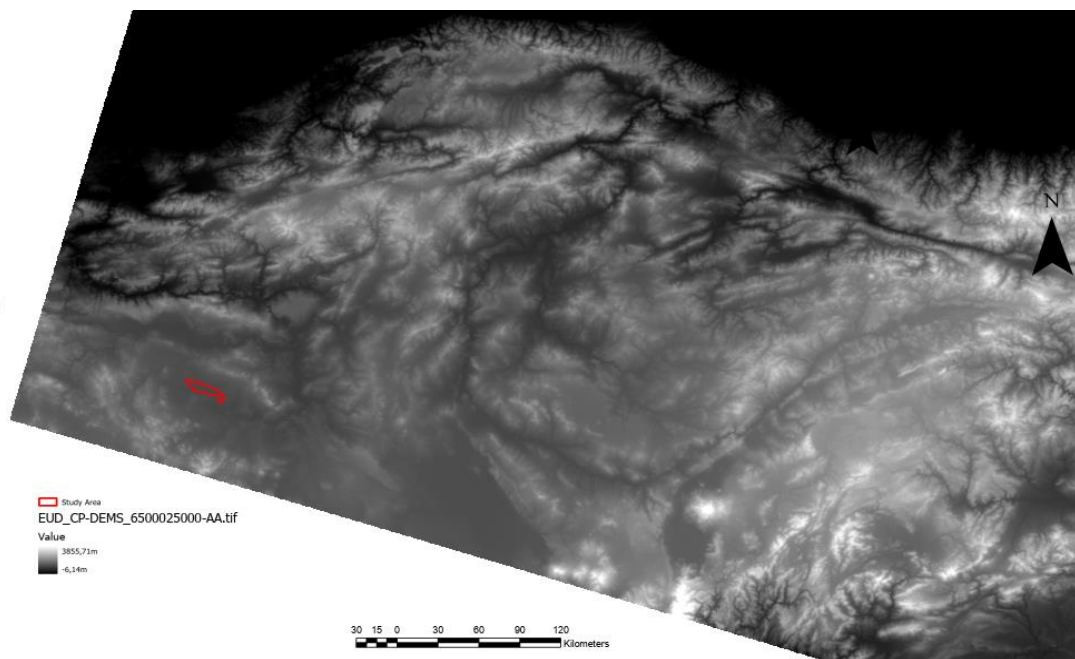


Figure 4.3. EUDEM (25m) covering the study area

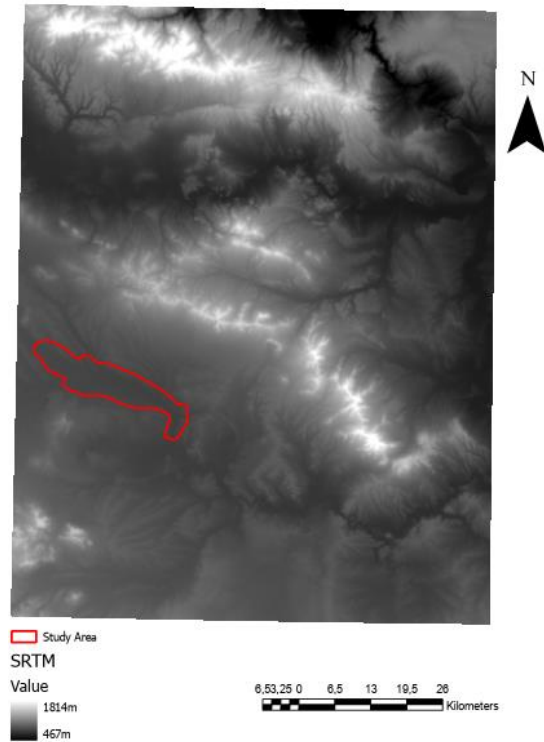


Figure 4.4. SRTM DEM (30m) covering the study area

The Digital Elevation Model (DEM) illustrated in Figure 4.5 has been sourced from the General Directorate of Mapping. This particular DEM offers a superior spatial resolution of 5 meters and has been measured in the same unit as the SRTM DEM. This particular dataset was generated through automated mapping of 30 cm stereo aerial photographs with a spatial resolution of 5 meters. At a 90% confidence interval, the vertical accuracy is  $\pm 3$  m [44].

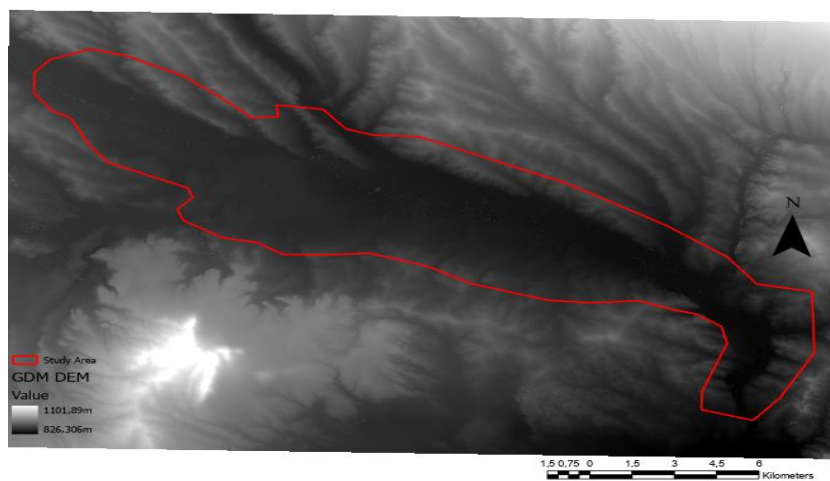


Figure 4.5. DEM from General Directorate of Mapping (5m)

The Digital Elevation Model (DEM) acquired from the SIUP is depicted in Figure 4.6. The DEM has a resolution of 5 meters and is based on the WGS 1984 coordinate system, measured in degree units (EPSG 4326). The data was acquired from SIUP, however, its origin can be attributed to the Ministry of Agriculture and Forestry, and the DSMs were generated using the adjusted stereo models. The DSM was utilized to classify point clouds and subsequently generate DTMs. Filtering algorithms were employed to produce DEMs in a 5-meter grid. The study area's data exhibits a vertical accuracy of 1,96 m, with a root mean square error of 0,26 at a 95% confidence interval [45, 46].

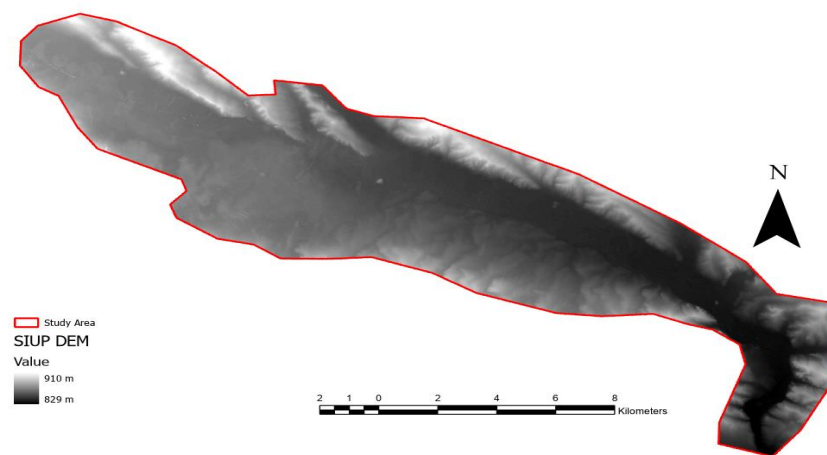


Figure 4.6. DEM from Sakaryabasi Irrigation Union Presidency (5m)

The datasets are available in various projection systems that do not adequately maintain the area's value. The EuDEM dataset employs the Lambert Azimuthal Equal Area projection. The study's objective of determining area values and conducting comparisons necessitates the selection of a suitable base projection system. In this regard, the EuDEM projection on ArcGIS software is chosen, and relevant reprojection tasks are subsequently executed. Furthermore, all DEM data that pertains to the study area has been clipped using polygon boundaries.

#### 4.1.2 DTM from Points

The DTM points generated by GDLRC were produced after the flight missions and have a 20-meter spacing across the study region, as illustrated in Figure 4.7. The accuracy of these points is 3 cm on both the X and Y axes and 5 cm on the Z axis. Figure 4.8 displays the elevation data that has been produced through the application of an interpolation

method (see Section 4.2.2) on 20-m resolution DTM points. The coordinate system used for this DTM dataset is consistent with the one applied in the previous section.

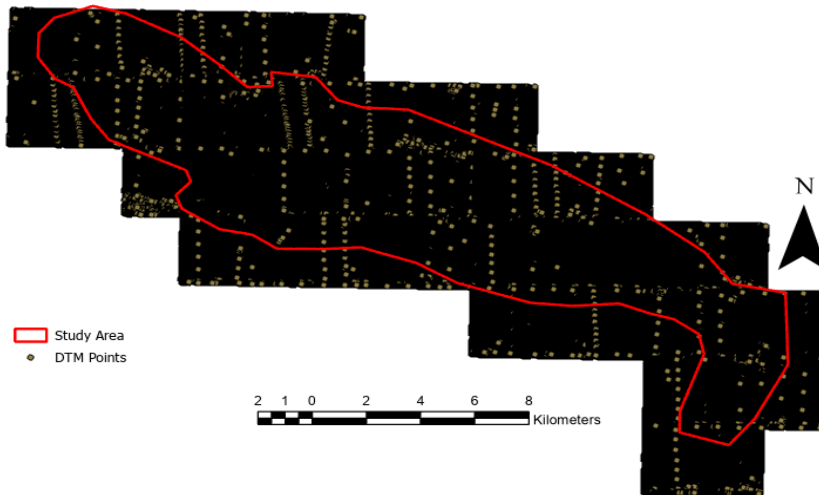


Figure 4.7. DTM points of the study area

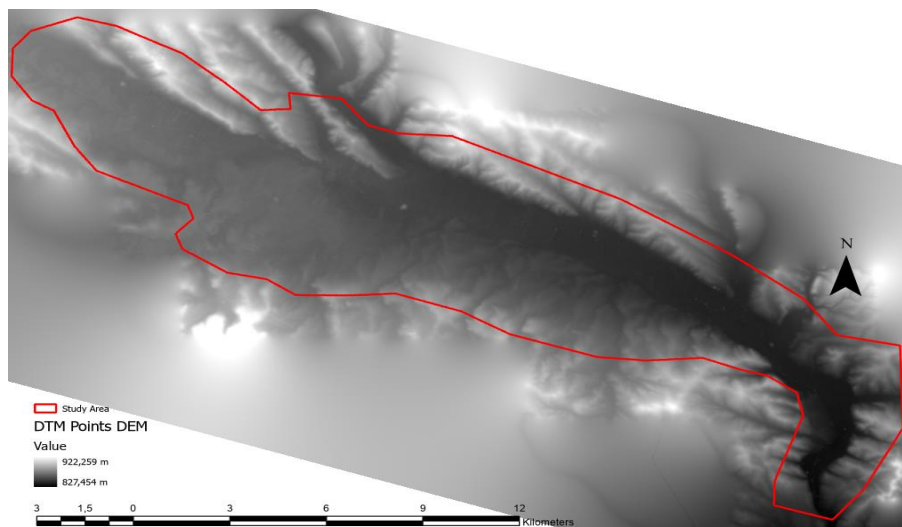


Figure 4.8. DTM generated from points using interpolation

### 4.1.3 Parcel Data

The study area and associated parcel data are shown in Figure 4.9. The parcel data was acquired from SIUP and subsequently modified to ensure seamless alignment with the DEM data. The registered area information in the parcel data indicates that this refers to a parcel of 9208 units, covering an area of 10.677,05 hectares. The GIS software, when applied in 2D, calculates the area to be 10.678,60 hectares. Evidently, a difference of 1,53

hectares exists between the area indicated on the title deed and that calculated from the geometric area.



Figure 4.9. Parcel data utilized.

## 4.2 Main Processing Steps Involved

The computation of accurate three-dimensional surface area and flow directions necessitates the utilization of DTM data to mitigate the impact of surface area differences that may arise as a result of variations in elevation across regions containing vegetation, structures, or other features. Therefore, the DEM data obtained from various sources may contain off-ground objects. To obtain a surface without any features that have an elevation above the terrain, DTM data was generated on Cloud Compare software using the Cloth Simulation Filter (CSF) plugin [47].

### 4.2.1 Cloth Simulation Filter (CSF)

The CSF plug-in has been developed with the purpose of separating ground and off-ground data from point clouds, as depicted in Figure 4.10. This add-on can be used with Cloud Compare according to several parameters set by the user, if necessary. This is expected to be useful for filtering points from a point cloud, in particular LiDAR data used for generating DTMs [48].

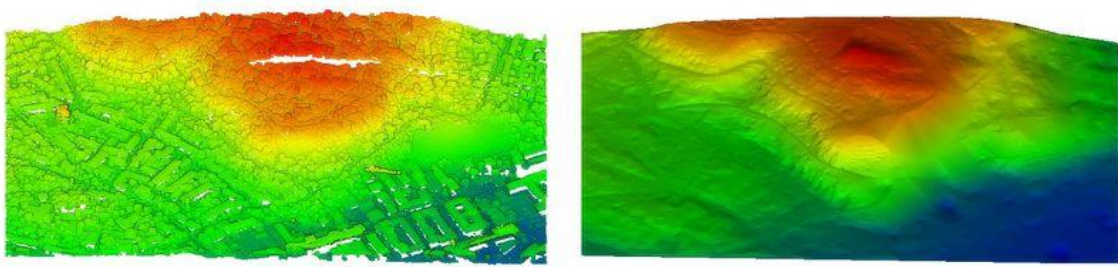


Figure 4.10. Generating DTM from DEM with CSF [47]

The algorithm involves the inversion of the initial point cloud, followed by the placement of new points on the surface (cloth) onto the inverted surface. Through an analysis of the correlation between the nodal points and their corresponding counterparts, a distinction is made between the ground and off-ground components, ultimately resulting in the determination of the final configuration of the point cloth (as depicted in Figure 4.11). Both the software and the plugin are available without cost, and the plugin's MATLAB code can be downloaded from MathWorks [49]. In order to utilize the plugin, it is necessary for the data to possess a projection that involves the meter units and identical x-y resolution values.

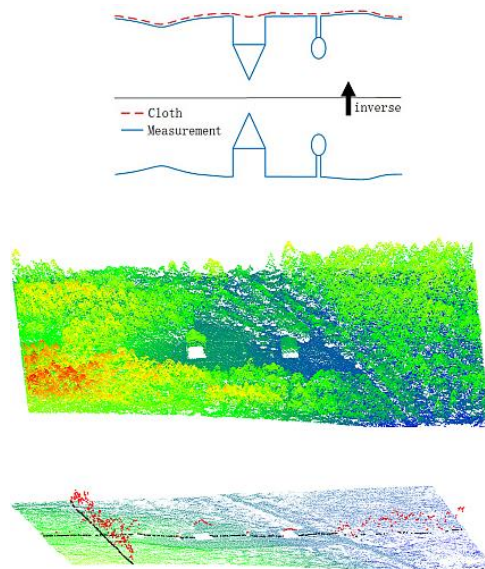


Figure 4.11. Principle of CSF [47]

#### 4.2.2 Interpolation

The present thesis necessitates the implementation of data interpolation for two distinct tasks. The first task involved utilizing the DTM points provided by GDLRC to produce a



raster DTM. Various methods exist for interpolating vector data to raster data, including Inverse Distance Weighted (IDW), Kriging, Topo-to-Raster, Nearest Neighbor, and Spline. These methods are commonly employed for generating raster datasets from vector data. The Topo-to-Raster technique has been found to provide superior accuracy in regions featuring streams and ridge lines, such as the study area under consideration [50, 51, 52]. The Topo-to-Raster technique is enhanced by its use of a drainage enforcement algorithm, which facilitates the removal of sinks during the generation of raster data [53]. The process employed in this study involved utilizing the Topo-to-Raster method to obtain an elevation model from DTM points.

The utilization of interpolation techniques can be employed in the second task to produce gapless DTM data. The process of generating a DTM involves obtaining both ground and off-ground raster data for a given area of interest, followed by the elimination of off-ground pixels. In order to address the gaps existing in the elevation data, an additional interpolation process must be employed. The gaps in the data can be filled using the interpolation method of plane fitting or the IDW fill method by computing the neighboring values. In cases where the error associated with the plane-fitting technique exceeds acceptable levels, the inverse distance-weighted (IDW) algorithm may be employed as an alternative approach.

### **4.3 Calculating Surface Area With DTM**

Using ArcGIS software, surface areas are calculated. The triangulated raster surface is used in the method to create the polygon's z-properties. From the raster cut in accordance with the polygon boundaries and the results obtained from this raster, the average z-value of the polygon is calculated. In this raster, each triangle's area is calculated by multiplying its surface area by the z-value of its midpoint. To determine the area of every triangle, these numbers are added together and divided by the total 3D area of the triangles [54, 55]. If surface data and polygon data are obtained, these tools can be used to compute surface areas and record them as a column in attribute tables [54, 55]. After that, parcel-by-parcel differences between surface area and planar area can be calculated.

Elevation models may exhibit abrupt holes in terrain that are referred to as sinks. Such errors in data can lead to inaccurate outcomes when computing surface areas and flow directions. So, it is important to remove these sink areas. A flow direction raster is

specifically required to eliminate these regions. The Topo-to-Raster interpolation technique incorporates an automatic sink cleaning process during the raster creation process, as previously mentioned. The computation of surface area involves the utilization of interpolation techniques. The available interpolation techniques comprise nearest neighbor, bilinear, and cubic convolution. The nearest neighbor approach utilizes the value of the closest cell to the center of the cell in question, without altering the original value of the input cells. The utilization of the bilinear method involves computing the output cell center as a weighted average of the four closest cell center values of the input. The weighted average of the four nearest cells becomes the weighted average of the 16 nearest cell center values for cubic convolution [56, 57].

#### **4.4 Calculating Flow Directions**

Flow directions are computed using the ArcGIS software. The direction of flow holds considerable importance in the planning and modeling of hydrological infrastructure. There exist both single and multiple techniques for performing calculations [58-62].

Three different methods can be used to calculate flow directions: the D-8 method, the Multiple Flow Direction Method (MFD), and the D-Infinity (DINF) method. [62] The D-8 algorithm enables the computation of the direction of flow with the greatest descent from a given cell to its eight adjacent cells. This method causes deflection on surfaces that are not in the direction of the grid. GD8 and iGD8 (improvements to GD8) methods were developed by Shin and Paik, which allow for the relocation of the cell where the deviations are collected [59].

The Multiple Flow Direction (MFD) algorithm, as tested by Qin et al. (2018), forecasts the direction of flow to be from a higher elevation cell to a lower elevation cell, thereby traversing all intermediate cells. A flow partitioning base is established from an approach based on local terrain conditions using the MFD method, and it is used to determine the fraction of downstream flow to all downhill neighbors. The D-Infinity (DINF) flow method is centered on the targeted cell; it determines the direction of flow as the steepest downward slope on the eight triangular surfaces created in the 3x3 cell window [61].



## 4.5 Processed Outputs

The process of generating a Digital Terrain Model (DTM), calculating the 3-dimensional surface area, and determining water flow direction necessitates the application of methods to the datasets, followed by a comparative analysis.

### 4.5.1 Generating DTM

The DEM data were processed to generate DTM data using the Cloud Compare CSF plugin, as illustrated in Figures 4.12 – 4.18. In this context, the term "ground point" refers to points that are anticipated to be located on the ground and are therefore expected to correspond to the Digital Terrain Model (DTM) points. Off-ground refers to points that possess varying Z values from ground level. Such points may be found atop a tree, building, crop, or other elevated structure. The selection of parameters during the generation of DTM data using the CSF plugin is dependent upon the resolution of the data.

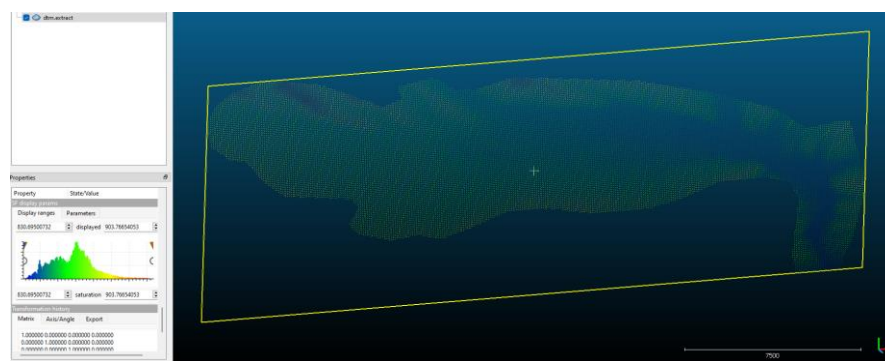


Figure 4.12. Point cloud of GDLRC DTM points

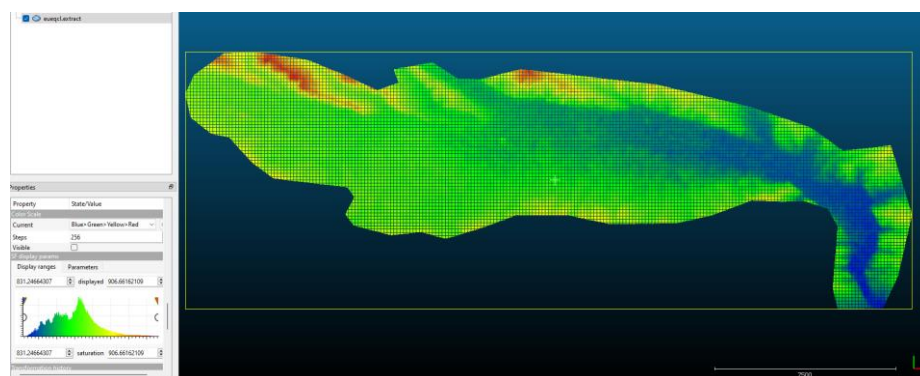


Figure 4.13. (a) Input point cloud of EuDEM

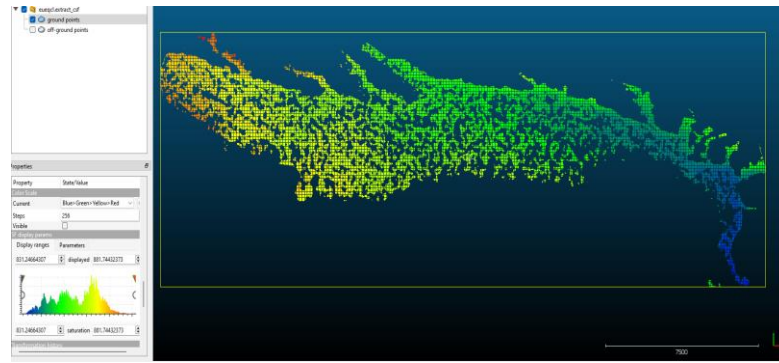


Figure 4.13. (b) Automatically extracted ground points of EUDEM

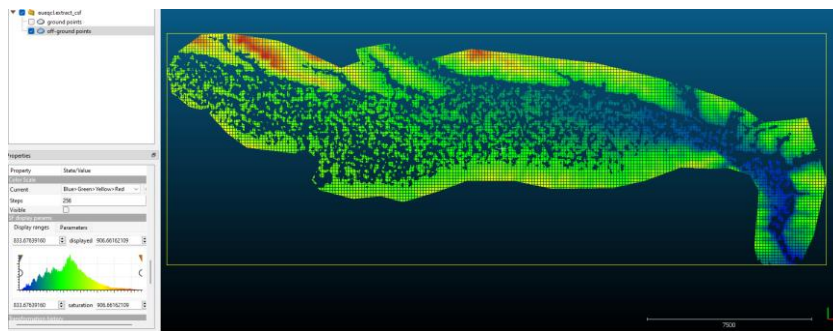


Figure 4.13. (c) Automatically extracted off-ground points of EUDEM

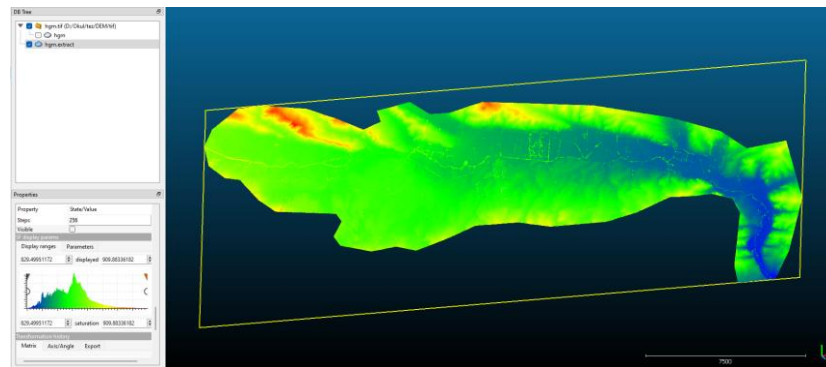


Figure 4.14. (a) Input point cloud of GDM DEM

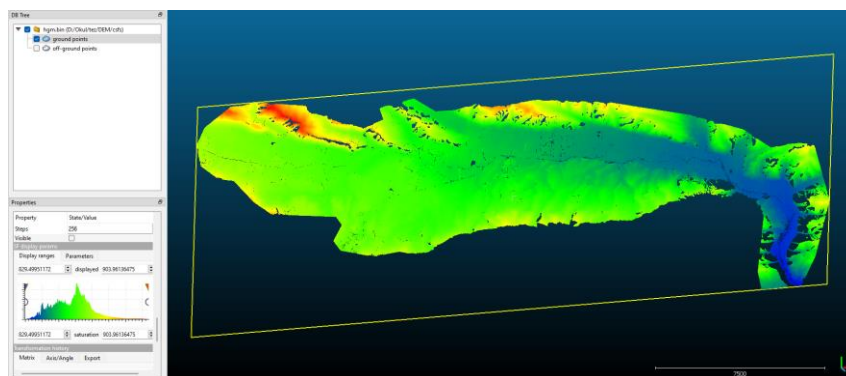


Figure 4.14. (b) Automatically extracted ground points of GDM DEM

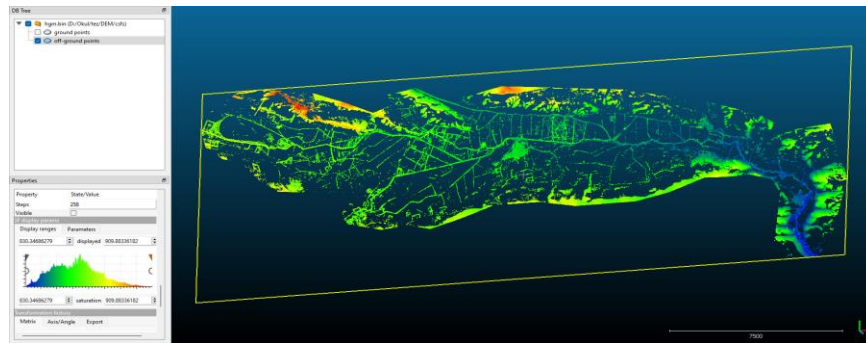


Figure 4.14. (c) Automatically extracted off-ground points.of GDEM

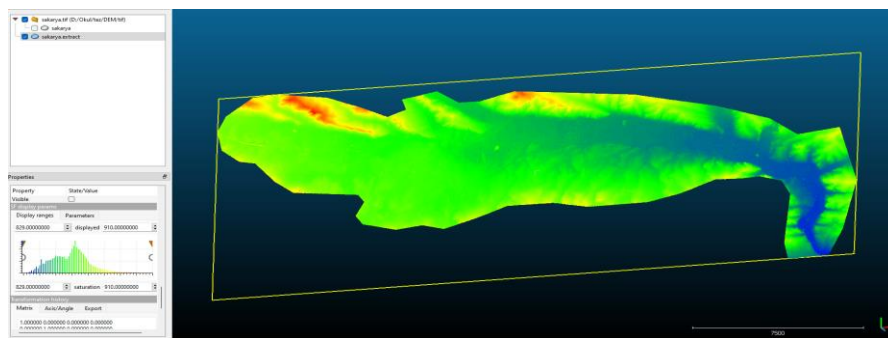


Figure 4.15. (a) Input point cloud of SIUP DEM

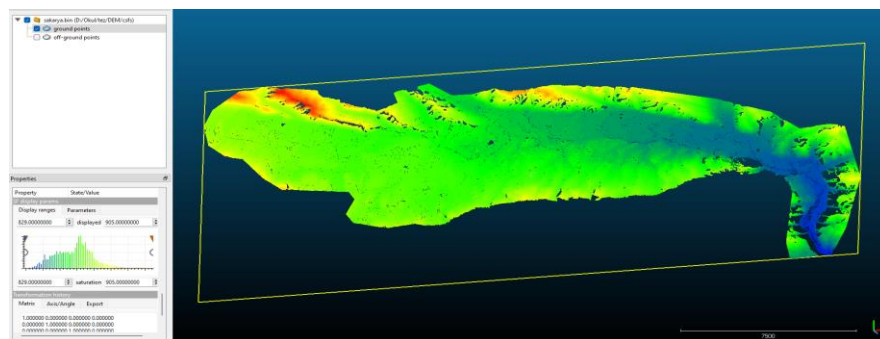


Figure 4.15. (b) Automatically extracted ground points of SIUP DEM

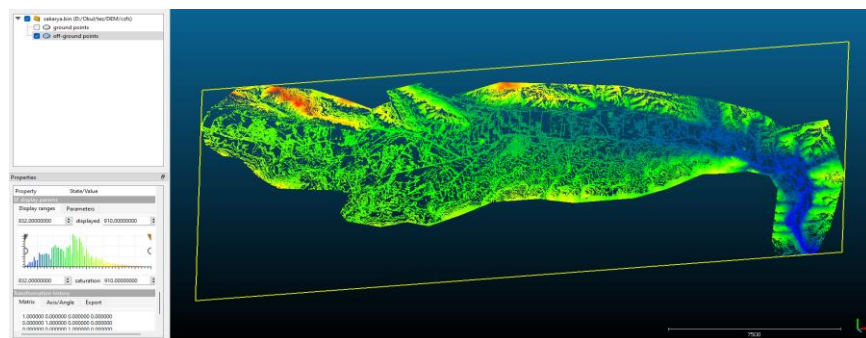


Figure 4.15. (c) Automatically extracted off-ground points of SIUP DEM

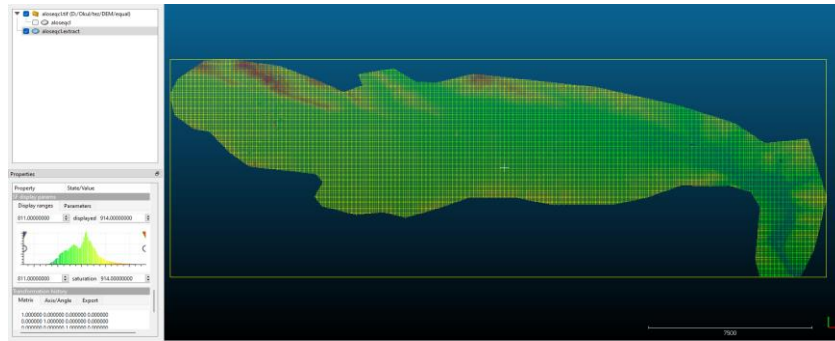


Figure 4.16. (a) Input point cloud of ALOS DEM

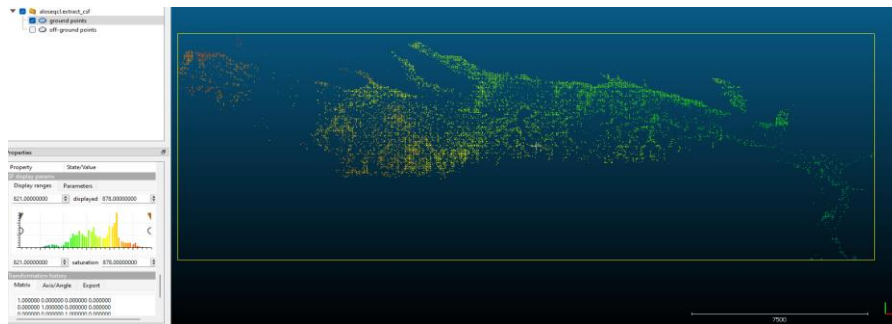


Figure 4.16. (b) Automatically extracted ground points of ALOS DEM

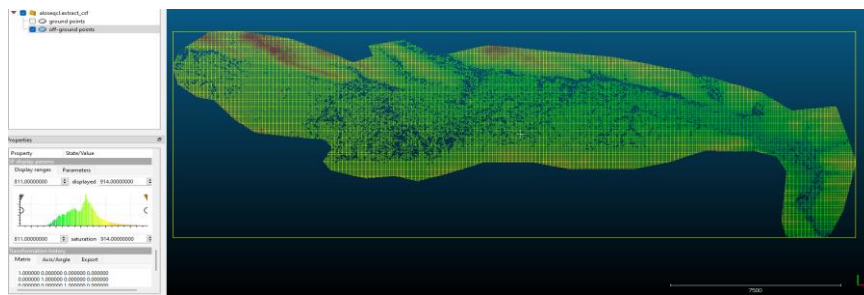


Figure 4.16. (c) Automatically extracted off-ground points of SIUP DEM

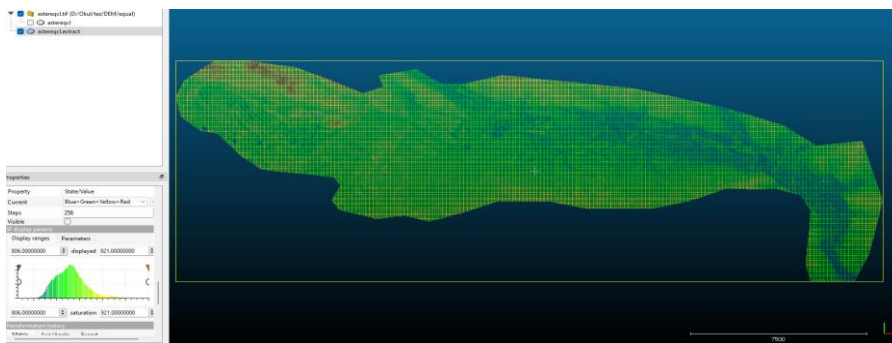


Figure 4.17. (a) Input point cloud of ASTER DEM



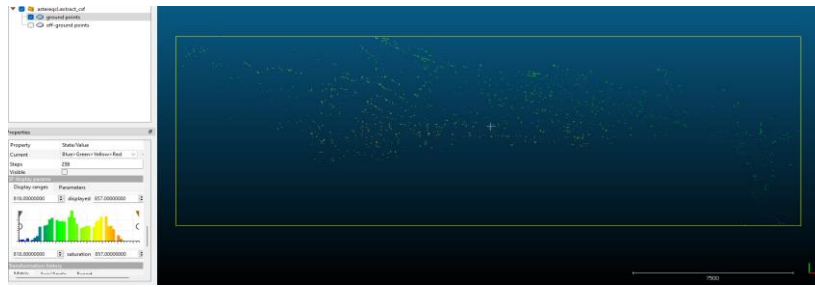


Figure 4.17. (b) Automatically extracted ground points of ASTER DEM

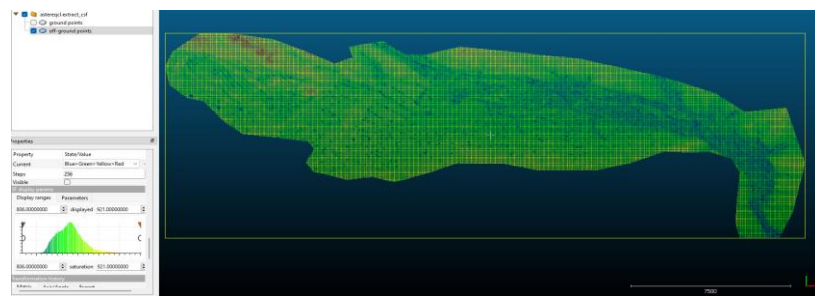


Figure 4.17. (c) Automatically extracted off-ground points of ASTER DEM

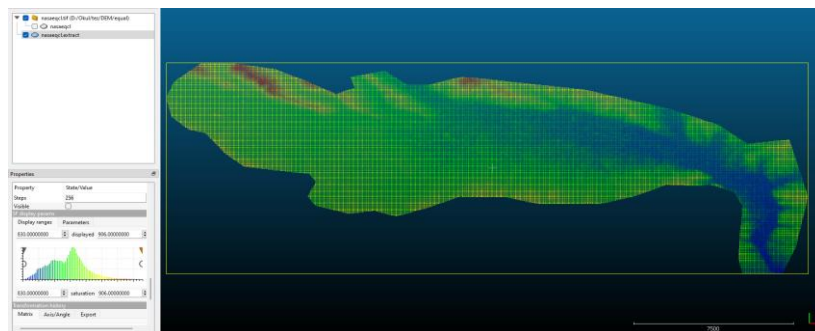


Figure 4.18. (a) Input point cloud of SRTM DEM

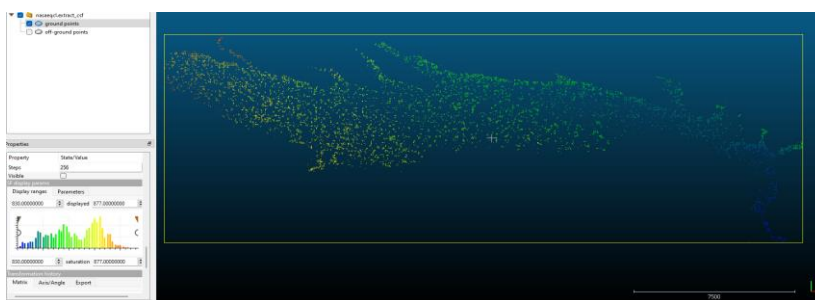


Figure 4.18. (b) Automatically extracted ground points of SRTM DEM

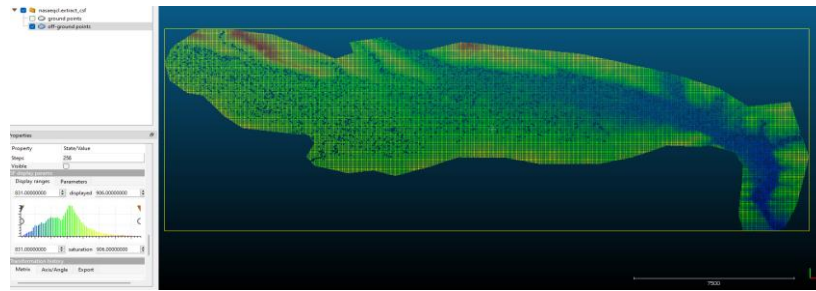


Figure 4.18. (c) Automatically extracted off-ground points of SRTM DEM

Prior to surface area calculations, it is important to consider the presence of gaps in the ground points raster resulting from the separation of data into ground and off-ground classes. These gaps must be addressed through the use of interpolation methods. The study area's GDLRC DTM points are depicted in Figure 4.19, while Figures 4.20-4.25 display the ground points for the DTM raster of the ground points that were observed.

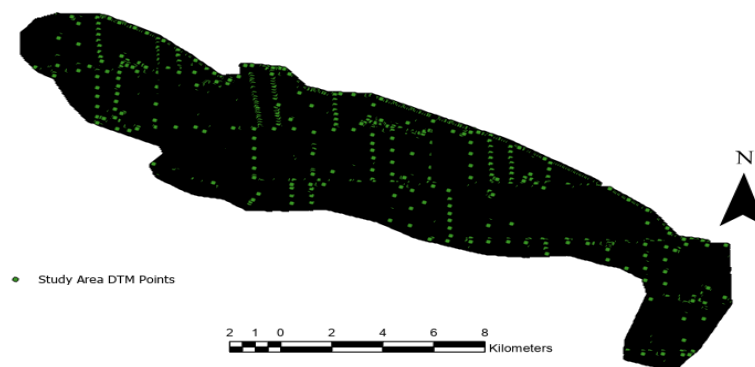


Figure 4.19. GDLRC DTM Points that Intersect with Study Area (Count 369.959)

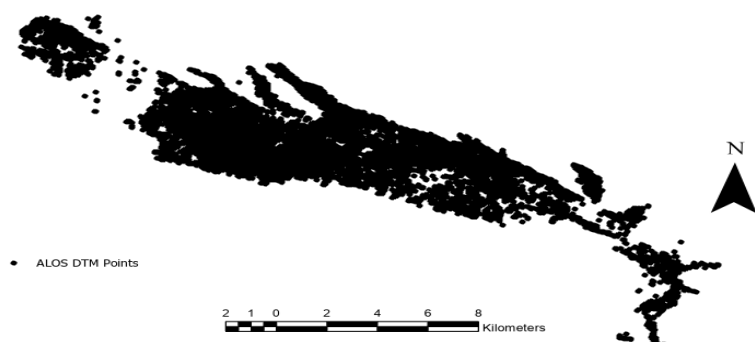


Figure 4.20. ALOS DTM Points (15.870 Ground Points)

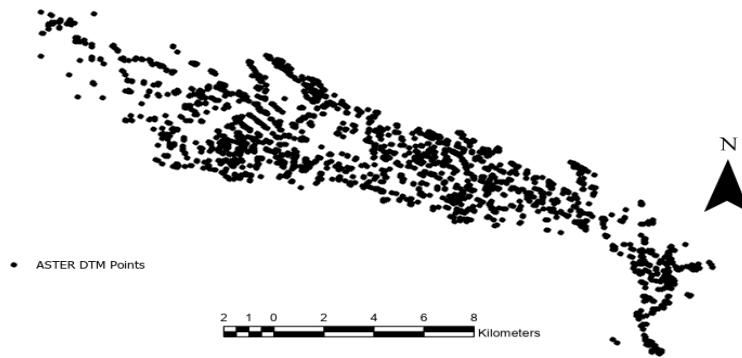


Figure 4.21. ASTER DTM Points (2.313 Ground Points)

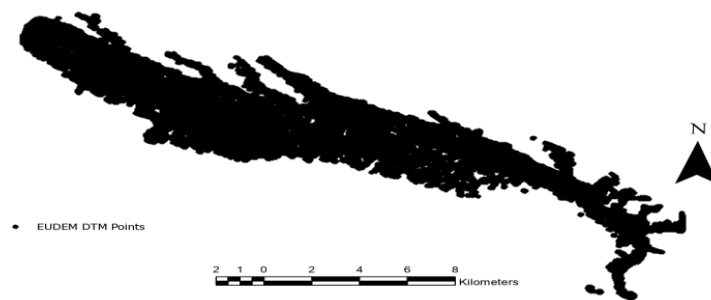


Figure 4.22. EUDEM DTM Points (27.230 Ground Points)

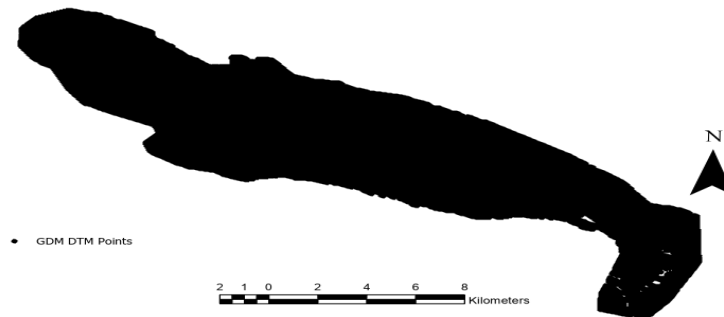


Figure 4.23. GDM DTM Points (4.357.709 Ground Points)

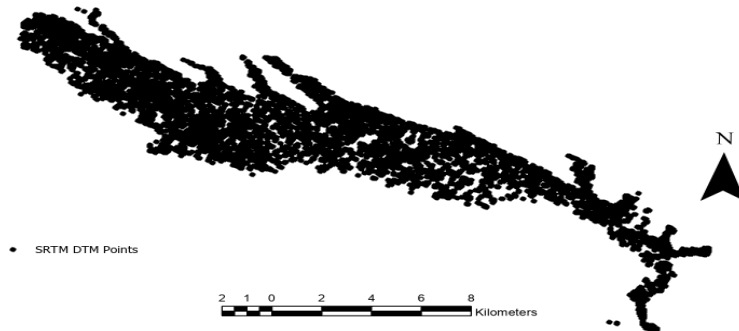


Figure 4.24. SRTM DTM Points (11.564 Ground Points)

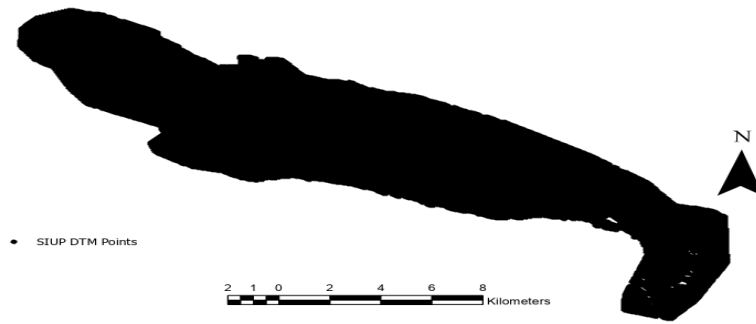


Figure 4.25. SIUP DTM Points (3.841.321 Ground Points)

Figures 4.26 – 4.32 depict the ground points that have been generated from the DTM raster in conjunction with the orthophoto. The utilization of GDM DEM has demonstrated the potential to produce ground points that are more exact and densely distributed. The SIUP DEM appears to be detailed, with proper DTM points. However, the GDM DEM exhibits a higher point density and more detail compared to the others.

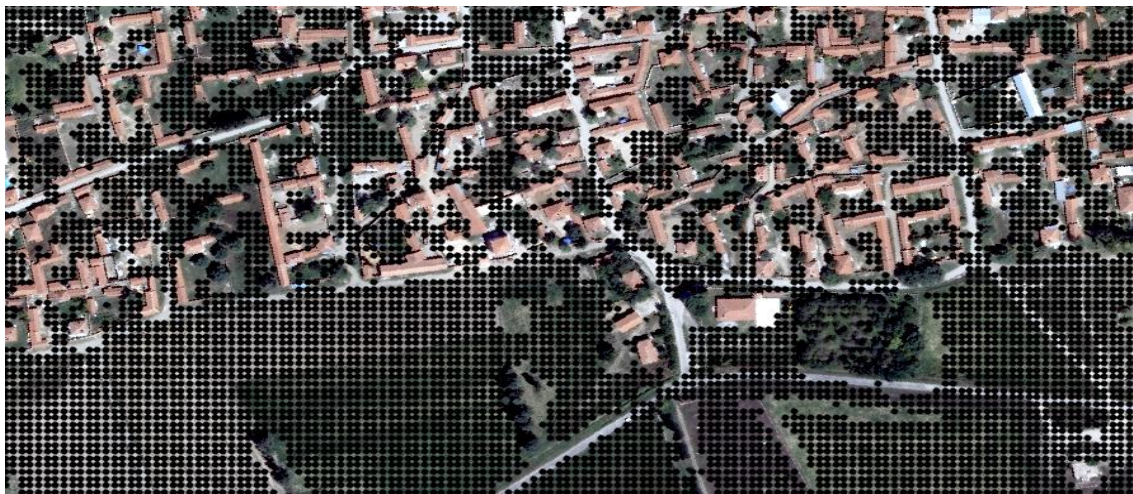


Figure 4.26. The orthophoto has been overlaid with GDM ground points.



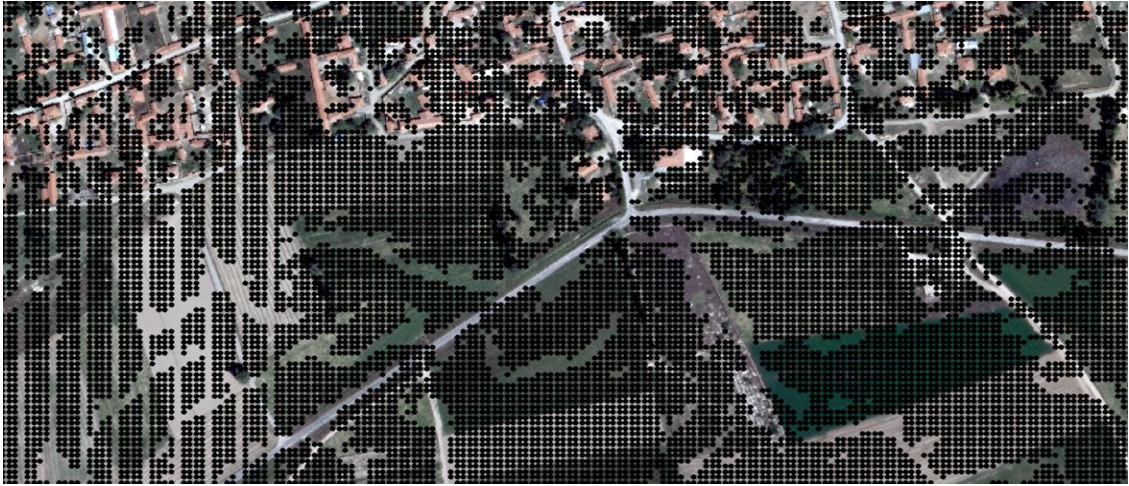


Figure 4.27. The orthophoto has been overlaid with SIUP ground points.



Figure 4.28. The orthophoto has been overlaid with EUDEM ground points.



Figure 4.29. The orthophoto has been overlaid with SRTM ground points.





Figure 4.30. The orthophoto has been overlaid with ALOS ground points.



Figure 4.31. The orthophoto has been overlaid with ASTER ground points.



Figure 4.32. The orthophoto has been overlaid with GDLRC ground points.

#### 4.5.2 Surface Area Calculation

Polygon vector data and DTM raster data were used to calculate 3D surface area with the bilinear method (Figure 4.33). The bilinear method is one of the most common techniques

used in image processing because its calculation methods are simpler than other interpolation methods [56, 57]. Raster surface-specific interpolation method that takes cell values from the four nearest cells, and GIS software has the capability to calculate surface area by the polygons with surface data. All vector polygons have a minimum-maximum-mean Z value, slope value, and surface area value from surface data where these two data intersect. This method provides a smoother surface.

Before calculating surface area, care was taken to ensure that the raster data and the parcel data overlapped completely. The parcels whose borders do not fully overlap with the raster data and the parcels with errors in their information were removed. It is ensured that parcels with topological errors such as overlapping are not included in the calculation. All Z values from the raster are used in calculating surface operations, and the Z factor is selected as 1.

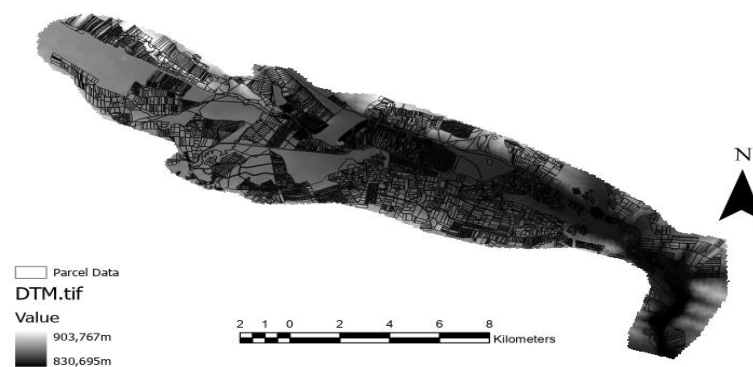


Figure 4.33. Parcel Data with DEM from DTM Points

#### 4.5.3 Flow Direction Outputs

The term "flow direction" refers to the direction in which water travels during precipitation or irrigation occurrences. The primary determinant is dependent on the slope of the terrain. This procedure was conducted to determine the parcels in which water accumulates. The flow directions depicted in Figure 4.34 -4.36 were derived by utilizing the DEM from DTM points with the highest density and flow accumulations derived from flow direction raster data.

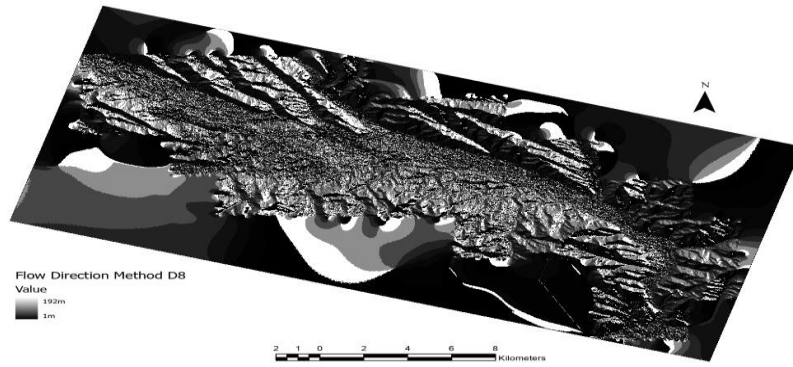


Figure 4.34. Flow direction with D8 Method

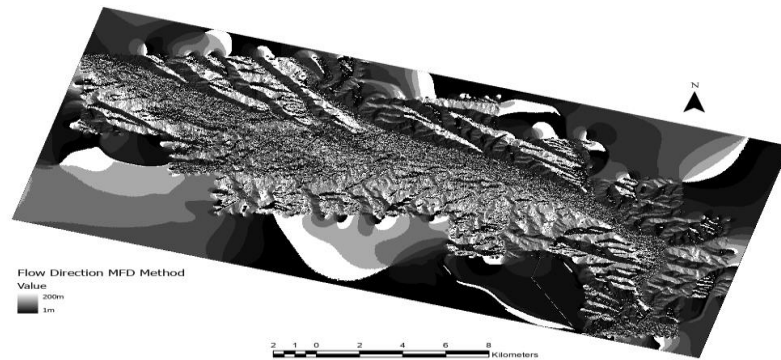


Figure 4.35. Flow direction with MFD Method

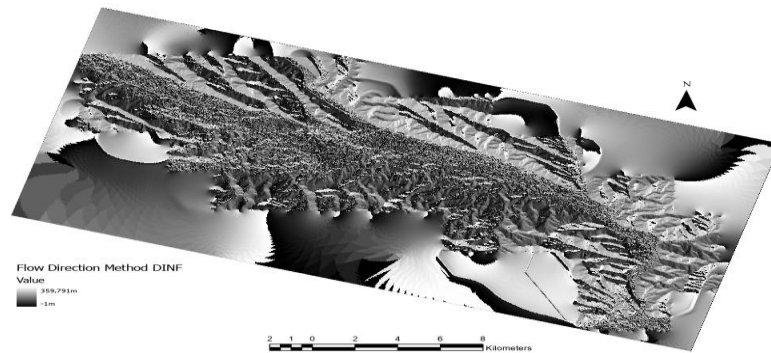


Figure 4.36. Flow direction with DINF Method

## 5. RESULTS AND DISCUSSION

This section is about calculated surface area and flow direction values, differences, comparisons, and discussions.

### 5.1 Comparisons Using Interpolated Surface Areas

The process of inspecting different DEM data involves the comparison of the information extracted. The study utilized a total of 9208 parcels for the related calculations, and the resulting values for the sum of absolute differences in hectares are presented in Table 5.1. The ASTER DTM exhibits the highest absolute difference between its surface area and geometric area when compared to other datasets. Subsequently, the aforementioned were succeeded by SIUP, GDM, ALOS, SRTM, EUDEM, and GDLCR. This analysis refers to the comparison between the surface measurements obtained through 2D and 3D techniques, facilitated by the outputs given in Section 4.5.

Table 5.1. Sum of absolute differences calculated in hectares (with gross errors)

<b>Input DTM Data</b>	<b>Geometric area vs. Registered Area</b>	<b>Surface Area vs. Geometric area</b>	<b>Surface Area vs. Registered Area</b>
ALOS	233,95	9,18	238,30
ASTER		83,84	314,65
EUDEM		6,21	235,28
GDM		9,84	236,83
SRTM		6,89	237,03
SIUP		21,81	243,71
GDLCR		5,82	235,09

The absolute sum of differences between surface area and registered area has the biggest value on ASTER DEM again, followed by SIUP, ALOS, SRTM, GDM, EUDEM, and GDLCR, as seen in Table 5.1. The observed dissimilarities appear to be comparatively minor when considering the overall extent of the study area. Nevertheless, in the context of agricultural analysis, they may hold considerable importance. Upon analysis of Table 5.1, it is evident that the minimal disparity observed at GDLRC regarding the surface area and registered area is 235 hectares. The study site under consideration is an agricultural region spanning an area of approximately 10.677,05 hectares. Inaccurate estimation of

water requirements for a portion of 235 hectares, which constitutes roughly 2,2% of the total area, could potentially result in substantial agricultural discrepancies across the entire country. Note that the calculation of the share of the irrigation water amount given to the farmers, the infrastructure planning for irrigation, and the agricultural supports depend on the registered area value. While the amount of water given affects crop yield, the amount of support given affects farmer income. Yield values and farmer incomes are very important for agricultural sustainability in our country [63]. Supports are also dependent on yield values. Therefore, the significance of the disparities between the registered area and 3D surface area is important, given that the mean size of farmland in our country is 6 hectares [63].

The calculation of the absolute sum of the difference between the geometric area and the registered area is performed independently, without any reliance on a DTM. These values are attributed to errors caused by outdated procedures employed in the computation of registered areas as well as errors made by humans. However, note that the determination of water allocation for agricultural irrigation is based on the information provided in the title deeds. Variations in the registered area on title deeds can result in variations in the amount of water allocated for irrigation purposes.

In areas where land is consolidated or cadastral renewal is performed, discrepancies between the geometric area and the registered area are minimal, but in other areas, discrepancies increase as a result of outdated information or human error. The absence of cadastral renewal or land consolidation in the aforementioned regions can be inferred from the fact that the parcel lot numbers are recorded as 0. There were 12 parcels with lot numbers, but because the geometric area and registered area are calculated differently due to the different shape of the data, these parcels are disregarded. Upon analyzing the variation between the geometric area and registered area of the study area presented in Table 5.2, it has been observed that discrepancies exceeding 1000 m<sup>2</sup> have the lot number of 0. This shows that there are data remaining from the cadastral parcel data obtained in the first cadastral registrations conducted in Türkiye.

Table 5.2. The parcel counts associated with the differences between registered area and geometric areas are presented on a village-by-village basis.

Village	Number of Parcels	The Number of Parcels with Calculated Differences			
		$\geq 0, < 50 \text{ m}^2$	$\geq 50, < 500 \text{ m}^2$	$\geq 500, < 1000 \text{ m}^2$	$\geq 1000 \text{ m}^2$
Abbashalimpasa	915	910	5	-	-
Aktas	388	384	4	-	-
Dikmen	1200	986	189	11	14
Eminekin	482	186	242	35	19
Gerenli	1134	276	780	51	27
Korhasan	2376	785	1397	117	77
Saithalimpasa	549	549	-	-	-
Selimiye	398	270	103	17	8
Yaveroren	439	305	116	10	8
Yıldızoren	1323	1319	4	-	-
Zaferhamit	4	4	-	-	-
<b>All</b>	<b>9208</b>	<b>5974</b>	<b>2840</b>	<b>241</b>	<b>153</b>

If there is no cadastral renewal, geometric area that we call geometric area can be different from registered area. So, in these areas, we should not use registered areas for agricultural or other processes that depend on the area. We can use geometric areas, but to have more accuracy, it is better to use surface area again. In Table 5.3, it is clear that we had significant differences between surface area and geometric area. In Table 5.4, the differences between the surface area and the registered area values are summarized according to the number of parcels for the DEM data.

Table 5.3 The parcel counts associated with the differences between the surface area and geometric area

Input DTM Data	The Number of Parcels with Calculated Differences			
	= 0	> 0, ≤ 100 m <sup>2</sup>	> 100 m <sup>2</sup> , ≤ 1000 m <sup>2</sup>	> 1000 m <sup>2</sup>
ALOS	51	8955	199	3
ASTER	-	8978	155	75
EUDEM	-	9053	154	1
GDM	-	9098	106	4
SRTM	13	9055	135	5
SIUP	689	8085	422	12
GDLCR	-	9149	58	1

Table 5.4: Parcel Counts for DEM based differences between Surface area and Registered Area

Input DTM Data	The Number of Parcels with Calculated Differences			
	= 0	> 0, ≤ 100 m <sup>2</sup>	> 100 m <sup>2</sup> , ≤ 1000 m <sup>2</sup>	> 1000 m <sup>2</sup>
ALOS	-	6750	2302	156
ASTER	-	6704	2278	226
EUDEM	-	6809	2249	150
GDM	-	6830	2223	155
SRTM	-	6790	2262	156
SIUP	-	6665	2387	156
GDLCR	-	6866	2190	152

Figures 5.1-5.7 show the calculated absolute differences between surface area and registered area by DEM data. The dark blue parcels show the biggest values for the absolute differences, and the light-yellow ones are the lowest values. This is due to the effect of the large area, which causes the larger polygons to have different and higher z values than the smaller ones.



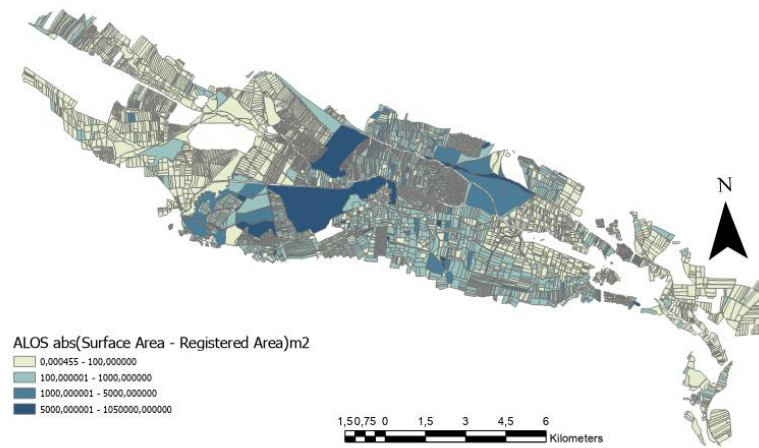


Figure 5.1. Surface area and registered area absolute differences for ALOS

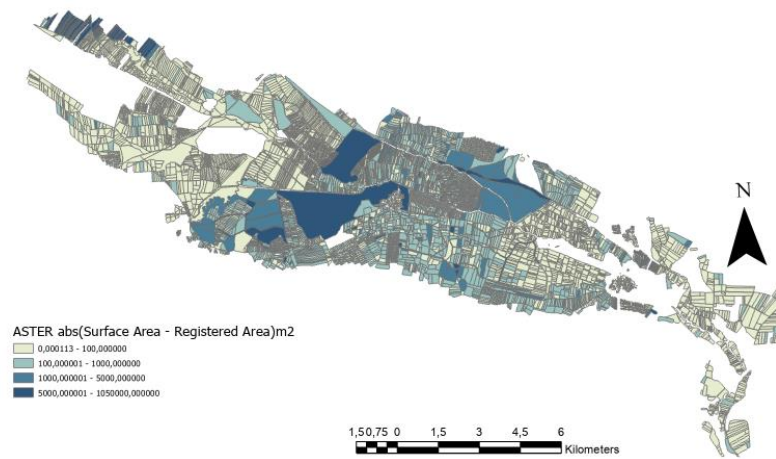


Figure 5.2. Surface area and registered area absolute differences for ASTER

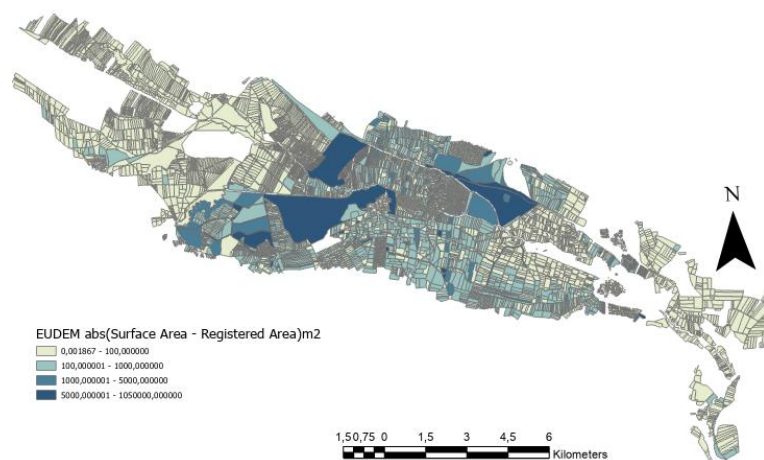


Figure 5.3. Surface area and registered area absolute differences for EUDEM

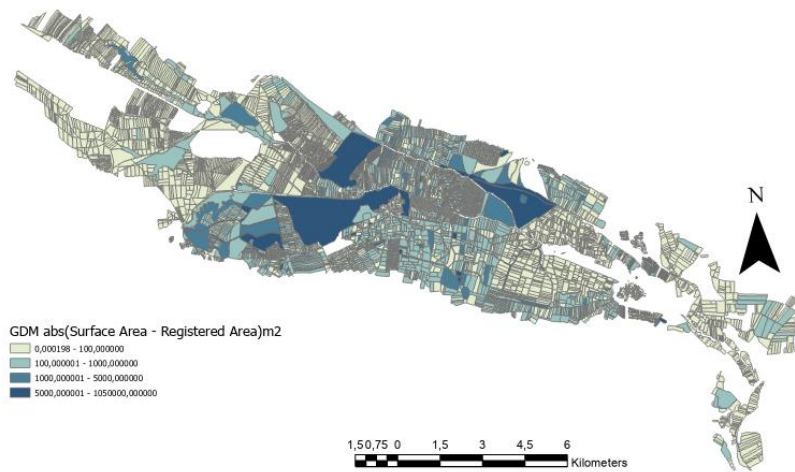


Figure 5.4. Surface area and registered area absolute differences for GDM

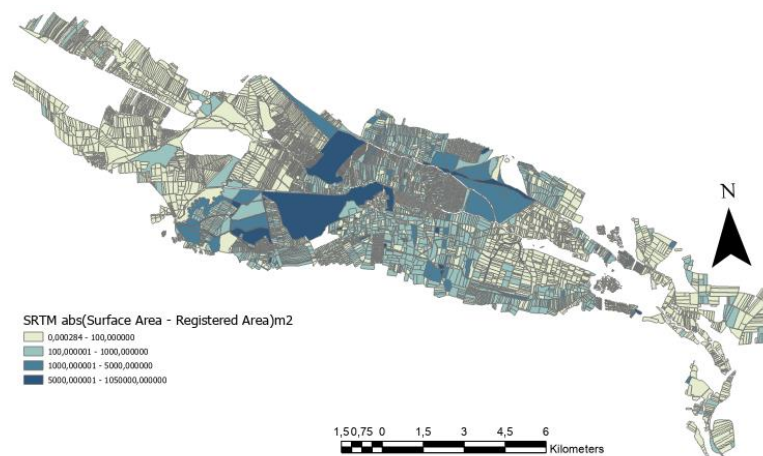


Figure 5.5. Surface area and registered area absolute differences for SRTM

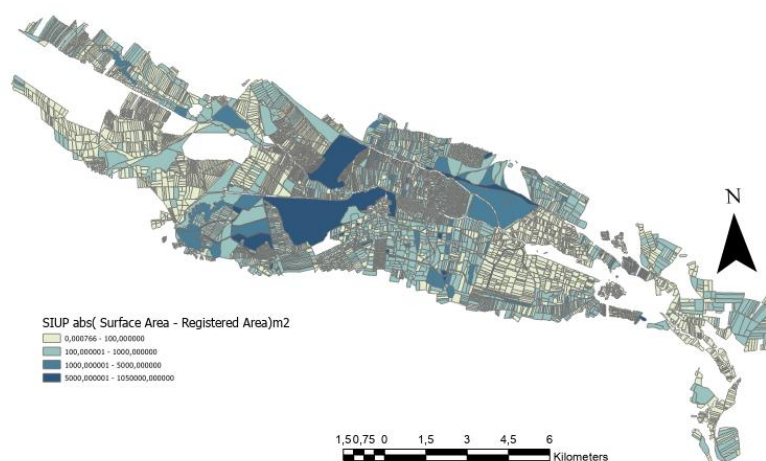


Figure 5.6. Surface area and registered area absolute differences for SIUP

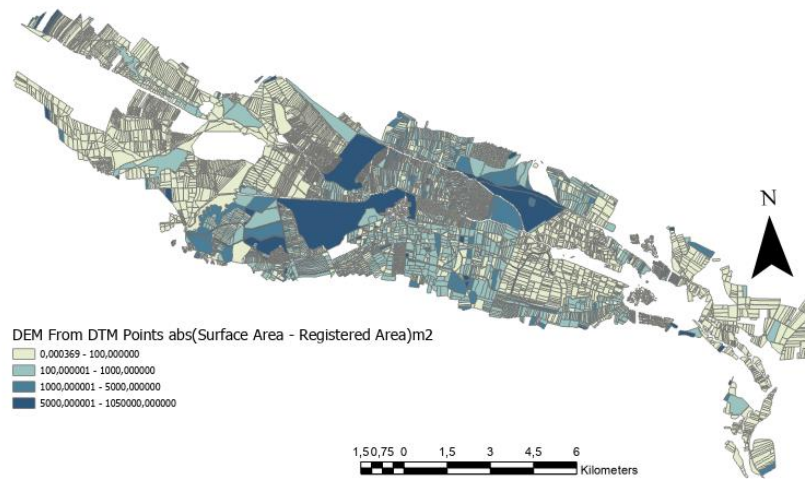


Figure 5.7. Surface area and registered area absolute differences for DTM points DEM

Although the discrepancies in individual areas may be minor, they can have major consequences for numerous agricultural domains. The yield value of a crop is influenced by various factors such as the quantity of water and fertilizer applied, the level of support provided to the farmer, irrigation infrastructure planning, and the budget allocated to the land. Additionally, the total area of the parcel can also impact real estate values. The impact of this phenomenon is expected to be more pronounced in regions where communal activities like irrigation agricultural unions are common. In regions characterized by greater topographic complexity, the contrast between the three-dimensional surface area and the two-dimensional planar area will exhibit a more confirmed extent. Thus, the aforementioned arguments will be impacted to a greater extent.

## 5.2 Flow Direction Calculations

The capabilities of GIS software are utilized for the computation of flow direction. The MFD method was used in this study to partition flow from the highest cell to all downslope neighbors [59]. In addition, the fact that the D8 method causes sink errors, the presence of structures such as water channels that may cause sink errors in the study area, in addition to these, the formation of -1 value, which is defined as meaningless in the data by DINF method, has shown that using the MFD method will achieve more accurate results. This method is also selected at the accumulation step with the integer output type for facilitating data for other required calculations. By integrating this information with parcel data, we are able to determine which polygon is more susceptible to the accumulation of water.

The results were compared with the values of DTM points and found to be consistent. The computation of infrastructure based on water catchment areas and flow patterns, coupled with the utilization of such information in determining the allocation of water per parcel for agricultural purposes, results in efficient water management.

The flow accumulation values (Figure 5.8) were matched with corresponding polygons, and subsequently, the flow accumulation values for the parcels were acquired as shown on Figure 5.9. This implies that the accumulations of water flow can be determined on a per-parcel basis.

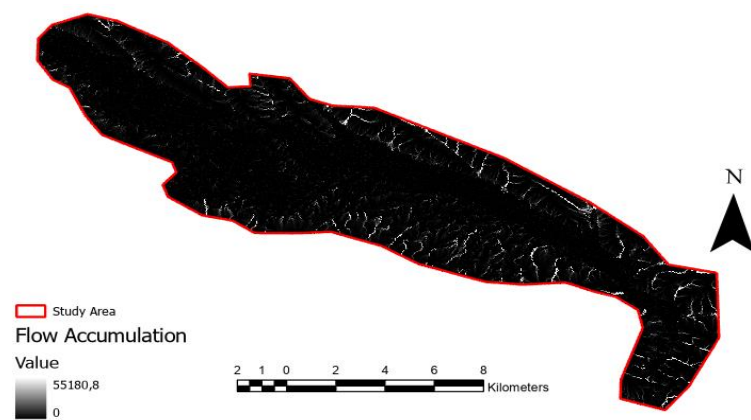


Figure 5.8. Flow Accumulation MFD Method



Figure 5.9. Flow accumulation with parcel data

Ensuring the precision of the DTM data is essential for the accurate determination of both the 3D surface area and the direction of flow. The significance of DTM data and its precision in the computation of surface area and flow direction, particularly in agricultural

domains, cannot be overstated. The utilization of DEM data in the computation of surface area and flow direction is subject to the influence of crop and other feature elevations, which can impact the resultant areas and directions. Therefore, the calculation of surface areas and flow directions is derived from DTM data. The flow accumulation raster map was derived from the flow directions raster map. The parcels on which water flow has accumulated were identified. When calculating irrigation water in a parcel unit area, it is important to consider the surface areas and accumulation amounts of the parcels where water accumulates. Therefore, optimizing water supply to the plant can potentially enhance yield outcomes by providing the precise amount of water required without excess or deficiency.

Tables 5.5 and 5.6 present the computed irrigation water quantities for crops on a 15-hectare scale in laboratory and field settings, respectively. The laboratory values presented in Table 5.5 indicate the necessary quantity of water that a plant must uptake throughout the growing season to achieve optimal productivity. The values displayed in Table 5.6 apply to the prevention of potential losses in regions where dripping and sprinkling water are utilized. These values are calculated based on various parameters such as soil moisture, evaporation, and infiltration, among others. The results obtained from laboratory calculations and field calculations exhibit disparities, as evidenced by the tables. Upon observation of Tables 5.5 and 5.6, it can be inferred that the values presented relate to a land area of 15 hectares. Consequently, it can be inferred that the aforementioned values will experience adjustments when implemented on a more extensive terrain, as exemplified by the 235-hectare variation observed in the previous section. Discrepancies between the surface area and planar area computations outlined in the thesis result in omissions in the irrigation water calculations. The utilization of surface area and flow accumulation computations for parcels can enhance the precision of water usage and increase yield.

Table 5.5: Irrigation water values for crops at 15ha in laboratory conditions

Crop	Amount of Water (m <sup>3</sup> )
Cereals	30 000
Sunflower	40 000
Orchard Gourd	40 000
Corn	50 000
Sugar Beet	70 000
Clover	70 000

Table 5.6: Irrigation water values for crops at 15 ha in field settings

Crop	Amount of Water (m <sup>3</sup> )
Cereals	34 020
Sunflower	45 360
Orchard Gourd	45 360
Corn	68 040
Sugar Beet	79 380
Clover	79 380

The utilization of flow directions is an effective means of developing an irrigation plan. By utilizing such data, it is possible to calculate the accumulation of water on specific parcels and subsequently adjust the amount of water to be allocated to those parcels. It is noteworthy that the quantity of water administered in agricultural irrigation has a significant impact on crop yields, as previously mentioned. The yield values are subject to direct influence from various factors, such as the food requirements of the country, the level of support provided to the farmers, and the degree of agricultural sustainability. The significance of agriculture has been highlighted again in light of the COVID-19 pandemic in recent years. It is essential to perform parcel-based calculations of 3D areas and determine surface flow directions in irrigation areas to ensure the effective use of water and the sustainability of agriculture. In areas where water accumulates due to elevation, incorporating the impact of precipitation and irrigation water into infrastructure planning can yield advantageous outcomes. Furthermore, in areas where water accumulates, the national water consumption might be optimized through reduced irrigation methods while simultaneously ensuring adequate water supply to meet the plant's requirements.

## 6. CONCLUSION

Türkiye is characterized by a topographically varying terrain as opposed to a primarily flat land structure. Despite this fact, the area values are incorporated in 2D within the title deeds, a legally binding document that contains information related to the area of the parcels. In cases where the terrain is flat, it is considered appropriate to include 2D area information in the title deed. However, in instances where the land is uneven, this approach may lead to undesirable outcomes such as loss of rights and inaccuracies in calculations. Furthermore, it is evident that in regions of Türkiye where cadastral renewal has not been conducted, there is a discrepancy between the registered area value on the title deed and the geometric area, even in cases where the land is flat.

The present study aimed to assess the suitability of 3D data-derived area measurements for determining water allocation per parcel for agricultural irrigation. Specifically, the study compared the calculated area values obtained from 3D data with the areas indicated on the title deeds. To achieve the stated objective, DEMs were obtained from publicly accessible data sources and institutions. Moreover, the information pertaining to the points of the DTM was obtained from the General Directorate of Land Registry and Cadaster. The 3-dimensional measurements of the parcels were obtained by utilizing elevation models and parcel data. Furthermore, the aforementioned data were utilized to perform computations regarding the flow orientations and the watershed regions essential for irrigation purposes.

According to the comparative analysis of the 3D area values obtained with the area values mentioned in the title deed and the 2D geometric area values, it has been observed that there exists a discrepancy of approximately 235 hectares between the cumulative area values of the title deeds and the computed 3D area value within the study area selected for agricultural irrigation in the Sakaryabasi region. The 235 hectares difference was determined for a region with relatively smooth terrain, but it is expected to be higher in the country's more rugged regions. In addition, an output was generated to determine the flow orientations and accumulation zones of water based on the topographical and irrigation plans. Note that the prevention and transfer of water accumulations to the stream in the study area were achieved through the implementation of engineering

structures constructed approximately half a century ago. However, new irrigation zones and in agricultural areas whose topography seriously changes after the earthquakes in Türkiye, also urbanism sector may greatly benefit from acquiring this knowledge.

Since the DTM point data indicates that there is a height difference of about 97 meters between the highest and lowest points, even in a relatively flat area, the calculation of the area data in three dimensions using these DTM points obtained from across the country will reveal differences on the basis of parcels. In this particular context, computations can be conducted utilizing the registered area in forthcoming assessments. These assessments may include, but are not limited to, property valuation, agricultural subsidies, land consolidation, and land reformation practices. In addition, future research into the value of agricultural irrigation zones where elevation data varies significantly and analyses of the effects of such disparities could be of interest.



## REFERENCES

- [1] U. Yildiz, M. Gurel, S. Kocaman Gökçeoglu and J Zevenbergen, Possible Negative Legal Impacts on Cadastral Work Due to Lack of Perception on Spatial Uncertainty, FIG Congress, **2022**.
- [2] E. E. Ergani and H. Celik, Tapu Bilgileri İle Kadastro Verileri Arasındaki Alan Farklılıkları, presented at TMMOB 6. Coğrafi Bilgi Sistemleri Kongresi, 23-25 Ekim 2019, Ankara, **2019**.
- [3] Fa. I. Hairuddin , A. R. A. Rasam , M. H. Razali, Development Of A 3d Cadastre Augmented Reality And Visualization In Malaysia, The International Archives of the Photogrammetry, Remote Sensing and Spatial Information Sciences, Volume XLVI-4/W3-2021, **2021**.
- [4] M. Karabin, D. Kitsakis, M. Koeva, G. Navratil, J. Paasch, J. Paulsson, N. Vučić, Ka. Janečka and A. Lisec, 3D Cadastre In The Case Of Engineering Objects, Such As Bridges and Road Viaducts 7th International FIG 3D Cadastre Workshop 11-13 October 2021, New York, USA, **2021**.
- [5] A. Zamzuri, I. Hassan and A. Rahman, Development Of 3d Marine Cadastre Data Model Based on Land Administration Domain Model, **2021**.
- [6] Z. Zhiming., F. V. Coillie, R. D. Wulf, E. M. D. Clercq and O. Xiaokun, Comparison of Surface and Planimetric Landscape Metrics for Mountainous Land Cover Pattern Quantification in Lancang Watershed, China. Mountain Research and Development 32(2): 213-25. **2012**.
- [7] <https://tagemsuet.tarimorman.gov.tr/> (Last Access 21/12/2022)
- [8] P. Zhang, W Ma, L. Hou, F. Liu and Q. Zhang, Study on the Spatial and Temporal Distribution of Irrigation Water Requirements for Major Crops in Shandong Province. Water 2022, 14, 1051, **2022**.
- [9] M. M. Haile and A. K. Abebe, GIS and Fuzzy Logic Integration In Land Suitability Assessment For Surface Irrigation: The case of Guder Watershed, Upper Blue Nile, Basin, Ethiopia, Applied Water Science (2022) 12: 240, **2022**.
- [10] K. C. Berber., F. B. Sanli and Basaraner M., Farkli Cözünürlüklerdeki Uydu Görüntüleri Ve Büyük Ölçekli Haritalardan Yararlanarak Ekili Alanların İzdüşüm Ve Yüzey Alanları Arasındaki İlişkinin İncelenmesi, VII. Uzaktan Algılama-Cbs Sempozyumu, 18-21 September 2018, Eskisehir, **2018**.
- [11] S. Temesgen, G. Mideksa and Seyoum T., Assessment of Irrigation Water Potential and Water Requirements of Selected Crops in The Wabe-Shebelle River Basin, Ethiopia, Water Resources and Irrigation Managementv.11, n. 1-3, p.47-65 2022, **2022**.
- [12] K. Toker, Türkiye’de Çeşitlerine Göre Kadastro Süreçlerinin Analizi, Tapu ve Kadastro Genel Müdürlüğü, Ankara, Türkiye, Proceedings of the World Cadastre Summit 2015, Istanbul, **2015**.

- [13] Yildiz, 2013, Türkiye Kadastrounun Mevcut Durumu ve Çok Amaçlı Kadastroya Yönelik Yeni Yaklaşımlar, Doctoral Thesis, July 2013, Trabzon, Karadeniz Technical University, Institute of Science and Technology, Department of Surveying Engineering, **2013**.
- [14] F. Doner, C. Biyik, O. Demir, Dünyada Üç Boyutlu Kadastro Uygulamaları, Jeodezi, Jeoinformasyon ve Arazi Yönetimi Dergisi 2011/2 Özel Sayı, **2011**.
- [15] R. Hajji, R. Yaagoubi, I. Meliana, I. Laafou and A. E. Gholabzouri, Development of an Integrated BIM-3D GIS Approach for 3D Cadastre in Morocco, ISPRS Int. J. Geo-Inf. 2021, 10(5), 351, **2021**.
- [16] M. Petronijević, N. Višnjevac, N. Prašćević and B. Bajat, The Extension of IFC For Supporting 3D Cadastre LADM Geometry, ISPRS Int. J. Geo-Inf. 2021, 10(5), 297; **2021**.
- [17] C Wang and C. Yu , Design, Development and Applicability Evaluation of a Digital Cartographic Model for 3D Cadastre Mapping in China, ISPRS Int. J. Geo-Inf. 2021, 10(3), 158; **2021**.
- [18] A. Balasubramanian, Digital Elevation Model (DEM) In GIS, Centre for Advanced Studies in Earth Science, University of Mysore, Mysore, Technical Report September, **2017**.
- [19] M. Ghandehari and B. P. Battenfield, Slope-Adjusted Surface Area Computations in Digital Terrain, PeerJ Preprints CC BY 4.0 Open Access rec: 30 Jul 2018, **2018**.
- [20] W. Figueira, R. Ferrari, E. Weatherby, A. Porter, S. Hawes and M. Byrne, Accuracy and Precision of Habitat Structural Complexity Metrics Derived from Underwater Photogrammetry, Remote Sens. 2015, 7, 16883–16900; **2015**.
- [21] J. S. Jenness, Calculating Landscape Surface Area from Digital Elevation Models, Wildlife Society Bulletin, 32(3), 829-839, **2004**.
- [22] J. Oksanen and T. Sarjakoski, Error propagation of DEM-based surface derivatives, Computers & Geosciences 31 (2005) 1015–1027/1016, **2005**
- [23] S. Xue, Y. Dang, J. Liu, Mi J., C. Dong, Y. Cheng, X. Wang and Wan J., Bias Estimation and Correction for Triangle-Based Surface Area Calculations, International Journal of Geographical Information Science, 30(11), 2155-2170, **2016**.
- [24] X. Shuqiang, D. Yamin, L. Jiping, M. Jinzhong, D. Chun, C. Yingyan, W. Xiaoqing and W. Jun, Surface Area Calculation for DEM-Based Terrain Model, August 2016 Survey Review 50(358):1-8, **2016**.
- [25] D. G. Tarboron, A New Method for The Determination of Flow Directions and Upslope Areas in Grid Digital Elevation Models, Water Resources Research, Vol. 33, No. 2, Pages 309-319, February, **1997**.
- [26] Soydan O., Niğde Ömer Halisdemir Üniversitesi Yerleşkesi Su Toplama Alanı ve Drenaj Ağlarının Archydro Yazılımı Kullanılarak Belirlenmesi, **2020**.
- [27] H.R.d.A Freitas, C. d.C Freitas, S. Rosim and J.R. d.F. Oliveira, Drainage Networks and Watersheds Delineation Derived From TIN-Based Digital Elevation Models / Computers & Geosciences 92 (2016) 21–37, **2016**.

- [28] M. J. Harrower, Geographic Information Systems (GIS) Hydrological Modeling In Archaeology: An Example From The Origins of Irrigation in Southwest Arabia (Yemen), *Journal of Archaeological Science*, **2010**.
- [29] Alkhuzai K. A. and Mohammed N. Z., Digital Elevation Model Analysis for Dam Site Selection Using GIS, *World Journal of Engineering Research and Technology WJERT*, **2022**.
- [30] Avand M., Kuriqi A., Khazaei M. and Ghorbanzadeh O., DEM resolution effects on machine learning performance for flood probability mapping, *Journal of Hydro-environment Research*, **2022**.
- [31] Ge Q., Zhang J., Chen, Z. and Li J., Application of Flow Velocity and Direction Measurement System in Slope Stability Analysis. *Water* 2021, 13, 700, **2021**
- [32] D. G. Tarboton, A New Method for The Determination Of Flow Directions And Upslope Areas In Grid Digital Elevation Models., *Water Resources Research* 33(2): 309-319. Copyright 1997 by the American Geophysical Union. Paper number 96WR03137. 0043-397/97/96WR-03137509.00, **1997**.
- [33] Sakaryabaşı Sulama Birliği Başkanlığı
- [34] Tarım Bilgi Sistemi <https://tbs.tarbil.gov.tr/> (last 10/05/2023)
- [35] Takaku J., Tadono T., Tsutsui K. and Ichikawa M., Validation Of 'Aw3d' Global Dsm Generated From Alos Prism, *SPRS Annals of the Photogrammetry, Remote Sensing and Spatial Information Sciences*, Volume III-4, 2016 XXIII ISPRS Congress, **2016**
- [36] Bayık Ç., Becek K., Mekik Ç., and Özendi M., On the Vertical Accuracy of the ALOS World 3D-30m Digital Elevation Model, *Remote Sensing Letters* 9(6):607-615, **2018**
- [37] D. B. Gesch, M. J. Oimoen, J. J. Danielson, and D. Meyer, Validation of the ASTER Global Digital Elevation Model version 3 over the conterminous United States, **2016**
- [38] ASTER Global DEM Validation Summary Report, **2009**
- [39] <https://hub.arcgis.com/content/ulisboa::eu-dem/about> (Last Access 10/05/2023)
- [40] EU-DEM Statistical Validation Report, **2014**
- [41] SRTM Mission Statistics, **2000**
- [42] Bildirici Ö., Üstün A., Uluğtekin N. Selvi H.Z., Buğdaycı İ. And Doğru A.Ö., SRTM Verilerine Dayalı Ülke Bazında 3"×3" Çözünürlüklü Sayısal Yükseklik Modelinin Oluşturulması:Proje Sonuçları, 2. Uzaktan Algılama ve Coğrafi Bilgi Sistemleri Sempozyumu, **2008**
- [43] Significant Topographic Changes in the United States, Accuracy Assessment of Elevation Data, USGS, **2019**
- [44] Sayısal Yüzey Modeli 5 m Seviye-0 (SYM5-L0), Harita Genel Müdürlüğü, (Last Access 10/05/2023)

- [45] [http://www.mescioglu.com.tr/Mescioglu\\_Harita\\_Birimi.pdf](http://www.mescioglu.com.tr/Mescioglu_Harita_Birimi.pdf) (Last Access 10/05/2023)
- [46] Information received from Mescioğlu Mühendislik ve Müşavirlik A.Ş.
- [47] CFS Plug-in, [http://www.cloudcompare.org/doc/wiki/index.php?title=CSF\\_\(plugin\)](http://www.cloudcompare.org/doc/wiki/index.php?title=CSF_(plugin)), (Last Access 02/01/2023)
- [48] Wuming Z., Jianbo Q., Peng W., Hongtao W., Donghui X., Xiaoyan W. and Guangjian Y., An Easy-to-Use Airborne LiDAR Data Filtering Method Based on Cloth Simulation, *Remote Sens.* 2016, 8(6), 501, **2016**.
- [49] CSF Matlab Code; <https://www.mathworks.com/matlabcentral/fileexchange/58139-csf-cloth-simulation-filter>, (Last Access 02/01/2023)
- [50] P.V. Arun, A Comparative Analysis of Different DEM Interpolation Methods, National Authority for Remote Sensing and Space Sciences the Egyptian Journal of Remote Sensing and Space Sciences, **2013**.
- [51] Colin Childs, Interpolating Surfaces In ArcGIS Spatial Analyst, Esri Education Services, **2004**
- [52] P. Jordan, Designing the DEM of the Base of the Swiss Plateau Quaternary Sediments, 6<sup>th</sup> ICA Mountain Cartography Workshop Mountain Mapping and Visualization, **2008**
- [53] How Topo to Raster works, <https://pro.arcgis.com/en/pro-app/latest/tool-reference/3d-analyst/how-topo-to-raster-works.htm>, (Last Access 02/01/2023)
- [54] Add Surface Information, <https://pro.arcgis.com/en/pro-app/latest/tool-reference/3d-analyst/add-surface-information.htm>, (Last Access 02/01/2023)
- [55] S. Karuppasamy, S. Kaliappan, R. Karthiga, C. Divya, Surface Area Estimation, Volume Change Detection in Lime Stone Quarry, Tirunelveli District Using Cartosat-1 Generated Digital Elevation Model (DEM), **2016**
- [56] <https://pro.arcgis.com/en/pro-app/latest/help/analysis/spatial-analyst/performing-analysis/cell-size-and-resampling-in-analysis.htm> (Last Access 02/01/2023)
- [57] S. Gao and V Gruev., Bilinear and Bicubic Interpolation Methods for Division of Focal Plane Polarimeters, *OSA Vol. 19, No. 27 / Optics Express*, 2011.
- [58] D. P. Patel and M. B. Dholakia, Identifying Probable Submergence Area of Surat City Using Digital Elevation Model and Geographical Information System, *World Appl. Sci. J.*, 9 (4): 461-466, **2010**
- [59] S. Shin and K. Paik, An improved method for single flow direction calculation in grid digital elevation models, WILEY, Copyright 2017 John Wiley & Sons, Ltd. Hydrological Processes, **2017**.

- [60] K. Paik, Global Search Algorithm for Nondispersive Flow Pathextraction, Journal of Geophysical Research, Vol. 113, F04001, 20081, **2008**.
- [61] C Qin, A. X. Zhu, T. Pei, B. Li, C. Zhou and L. Yang, An Adaptive Approach to Selecting a Flow Partition Exponent for A Multiple Flow Direction Algorithm, International Journal of Geographical Information Science 21(4): 443-458, **2007**.
- [62] Flow Direction (Spatial Analyst) ArcPro, <https://pro.arcgis.com/en/pro-app/latest/tool-reference/spatial-analyst/flow-direction.htm> (Last Accessed 10/06/2023)
- [63] G. Keskin, G. Kaplan and H. Başaran, Turkiye’de Aile Ciftciligi, İş Gucu Produktivitesi ve Sürdürülebilirlik, Harran Tarım ve Gıda Bilimleri Dergisi (2017) 21(2): 209-218, Research Article **2017**.

## **APPENDICES**

Attach 1 - Thesis Derived Publications

### **Attach 1 - Thesis Derived Publications**

A. I. Yavuz, A. O. Ok, Comparative Test of Digital Elevation Models to Accurately Predict the Surface Areas of Crop Lands in The Eskisehir - Cifteler Irrigation Zone, International Symposium On Applied Geoinformatics, Chania,Crete, Greece **2022**